JPEDAV (2010) 31:113–134
DOI: 10.1007/s11669-009-9643-6
1547-7037 ©ASM International

Thermodynamic Assessment of the Fe-Mn-O System

Lina Kjellqvist and Malin Selleby

(Submitted September 9, 2009; in revised form November 1, 2009)

The C-Cr-Fe-Ni-O system has recently been studied with the intention to thermodynamically describe the influence of oxygen on high alloyed steels. In this study the ternary Fe-Mn-O system is assessed and part of the binary Mn-O system is reassessed. α- and β-hausmannite (Mn_3O_4) were earlier described as stoichiometric phases, but are here described using the compound energy formalism with a four sublattice model to be consistent with the preceding study of the Cr-Fe-Ni-O spinel. The liquid phase is assessed using the ionic two-sublattice model. Good agreement between calculated and experimental values is achieved.

Keywords CALPHAD, Fe-Mn-O system, thermodynamic modelling

1. Introduction

In a preceding study the C-Cr-Fe-Ni-O system[1,2] was described. It is a basic system for describing stainless steels. In this study the Fe-Mn-O system is assessed, a first step towards a consistent C-Cr-Fe-Mn-Ni-O database. In the present work both the metallic and the oxide liquid are modelled using the ionic two-sublattice model.[3,4] The ionic two-sublattice liquid model was developed within the framework of the compound energy formalism (CEF),[5] which is used to describe phases using two or more sublattices and is widely used in CALPHAD assessments.[6,7]

The Fe-O system was assessed by Sundman,[8] and later modified by Selleby and Sundman[9] (ionic liquid), Kowalski and Spencer[10] (fcc and bcc) and Kjellqvist et al.[1] (hematite). This modified description of Sundmans assessment is used in this study. The Mn-O system has been assessed by Grundy et al.,[11] and is here accepted after slight modifications. Grundy et al. described α- and β-hausmannite (Mn_3O_4) as stoichiometric phases where each component can reside in only one sublattice, thus without the possibility to describe any degree of inversion. Those phases are now treated using a more complex model, where the degree of inversion and also the deviation from stoichiometry are described. In their model for the ionic liquid they use a Mn^{+3} species which now is replaced by a neutral $MnO_{1.5}$ species equivalent to the description of the Fe-O system. For the third binary, Fe-Mn, the assessment of Huang[12] is accepted without modification. The ternary system, Fe-Mn-O, has been assessed by Weiland,[13] but is reassessed in this work. Weiland used a different description of the Mn-O system and the α- and β-spinel phases were modelled as stoichiometric phases with respect to oxygen. Pelton et al.[14] performed an assessment on the Fe_3O_4-Mn_3O_4 system.

Some phases undergo a magnetic transition characterized by a λ-peak in the heat capacity curve. The magnetic contribution to the Gibbs energy is given by a model proposed by Inden[15] and adapted by Hillert and Jarl.[16]

Lina Kjellqvist and **Malin Selleby**, Materials Science and Engineering, KTH, SE-100 44, Stockholm, Sweden. Contact e-mail: lina@mse.kth.se.

2. Thermodynamic Models

2.1 Liquid

Grundy et al.[11] applied the ionic two-sublattice liquid model[3,4] to the Mn-O system, using the formula $\left(Mn^{2+}, Mn^{3+}\right)_P\left(O^{2-}, Va^{Q-}\right)_Q$. The liquid phase in the Fe-O system was first modelled with $\left(Fe^{2+}, Fe^{3+}\right)_P\left(O^{2-}, Va^{Q-}\right)_Q$,[8] but later Fe^{3+} was replaced by a neutral species, $FeO_{1.5}$.[9] This change was imposed by an equivalent change for Al-containing system where Al^{3+} was replaced by $AlO_{1.5}$ in order to better control the unwanted reciprocal miscibility gaps that occurred in e.g. Al_2O_3-CaO-SiO_2. However, even though a new model for liquid Al_2O_3 (without $AlO_{1.5}$) has been developed,[17] the $FeO_{1.5}$ species has been kept. In the present work the formula $\left(Fe^{2+}, Mn^{2+}\right)_P\left(O^{2-}, Va^{Q-}, FeO_{1.5}, MnO_{1.5}\right)_Q$ will be used. P and Q is the number of sites on each sublattice. P and Q vary so that electroneutrality is maintained. The same model can be used both for metallic and oxide melts. At low levels of oxygen, the model becomes equivalent to a substitutional solution model between metallic atoms. The Gibbs energy of the liquid phase is expressed by:

$$\begin{aligned} G_m = {} & y_{Fe^{2+}} y_{O^{2-}} {}^{o}G_{Fe^{2+}:O^{2-}} + y_{Mn^{2+}} y_{O^{2-}} {}^{o}G_{Mn^{2+}:O^{2-}} \\ & + Q y_{Va^{Q-}} \left(y_{Fe^{2+}} {}^{o}G_{Fe^{2+}:Va^{Q-}} + y_{Mn^{2+}} {}^{o}G_{Mn^{2+}:Va^{Q-}}\right) \\ & + Q\left(y_{FeO_{1.5}} {}^{o}G_{FeO_{1.5}} + y_{MnO_{1.5}} {}^{o}G_{MnO_{1.5}}\right) \\ & + RTP\left(y_{Fe^{2+}} \ln\left(y_{Fe^{2+}}\right)\right) + y_{Mn^{2+}} \ln\left(y_{Mn^{2+}}\right) \\ & + RTQ\left(y_{O^{2-}} \ln\left(y_{O^{2-}}\right) + y_{Va^{Q-}} \ln\left(y_{Va^{Q-}}\right)\right. \\ & \left. + y_{FeO_{1.5}} \ln\left(y_{FeO_{1.5}}\right) + y_{MnO_{1.5}} \ln\left(y_{MnO_{1.5}}\right)\right) + {}^{E}G_m \end{aligned} \quad \text{(Eq 1)}$$

where y denotes the site-fraction and ${}^{E}G_m$ is the excess Gibbs energy which depends on the interaction between species within each sublattice. The interaction parameters used in this assessment are the following:

$$
\begin{aligned}
{}^{E}G_m = {} & y_{Fe^{2+}}y_{Mn^{2+}}y_{O^{2-}}\left({}^{0}L_{Fe^{2+},Mn^{2+}:O^{2-}} + {}^{1}L_{Fe^{2+},Mn^{2+}:Va}(y_{Fe^{2+}} - y_{Mn^{2+}})\right) \\
& + Qy_{Va}^{2}y_{Fe^{2+}}y_{Mn^{2+}}\left({}^{0}L_{Fe^{2+},Mn^{2+}:Va} + {}^{1}L_{Fe^{2+},Mn^{2+}:Va}(y_{Fe^{2+}} - y_{Mn^{2+}})\right) \\
& + y_{Va}y_{Fe^{2+}}y_{O^{2-}}\left({}^{0}L_{Fe^{2+}:O^{2-},Va} + {}^{1}L_{Fe^{2+}:O^{2-},Va}(y_{O^{2-}} - y_{Va})\right) \\
& + y_{Va}y_{Mn^{2+}}y_{O^{2-}}\left({}^{0}L_{Mn^{2+}:O^{2-},Va} + {}^{1}L_{Mn^{2+}:O^{2-},Va}(y_{O^{2-}} - y_{Va})\right) \\
& + y_{Fe^{2+}}y_{O^{2-}}y_{FeO_{1.5}}\left({}^{0}L_{Fe^{2+}:O^{2-},FeO_{1.5}} + {}^{1}L_{Fe^{2+}:O^{2-},FeO_{1.5}}(y_{O^{2-}} - y_{FeO_{1.5}})\right) \\
& + y_{Mn^{2+}}y_{O^{2-}}y_{FeO_{1.5}}{}^{0}L_{Mn^{2+}:O^{2-},FeO_{1.5}} + y_{Mn^{2+}}y_{O^{2-}}y_{MnO_{1.5}}{}^{0}L_{Mn^{2+}:O^{2-},MnO_{1.5}} \\
& + Qy_{Va}(y_{Fe^{2+}}y_{FeO_{1.5}}{}^{0}L_{Fe^{2+}:FeO_{1.5},Va} + y_{Fe^{2+}}y_{MnO_{1.5}}{}^{0}L_{Fe^{+2}:MnO_{1.5},Va} \\
& + y_{Mn^{2+}}y_{FeO_{1.5}}{}^{0}L_{Mn^{2+}:FeO_{1.5},Va} + y_{Mn^{2+}}y_{MnO_{1.5}}{}^{0}L_{Mn^{2+}:MnO_{1.5},Va})
\end{aligned}
\qquad \text{(Eq 2)}
$$

A colon is used to separate species on different sublattices and a comma is used to separate species on the same sublattice.

2.2 Spinel: Cubic and Tetragonal

There are two types of spinel phases in the Fe-Mn system; cubic and tetragonal spinels (Strukturbericht $H1_1$ for cubic spinel). Hausmannite (Mn_3O_4) is a tetragonal spinel (α-Mn_3O_4) at low temperatures and transforms to a cubic spinel (β-Mn_3O_4) at higher temperatures. α-Mn_3O_4 dissolves small amounts of Fe, while β-Mn_3O_4 extend up to magnetite (Fe_3O_4). The tetragonal distortion originates from the Jahn-Teller distortion[18] of octahedral sites occupied by Mn^{3+} ions.

Dorris and Mason[19] found that α- and β-Mn_3O_4 have different ionic configuration. They believe that α-Mn_3O_4 has the same ionic configuration as cubic Fe_3O_4: $(Mn^{2+}, Mn^{3+})_1\ (Mn^{2+}, Mn^{3+})_2(O^{2-})_4$, while in the case of β-Mn_3O_4 Mn^{2+} resides on tetrahedral sites and Mn^{2+}, Mn^{3+} and Mn^{4+} on octahedral sites: $(Mn^{2+})_1(Mn^{2+}, Mn^{3+}, Mn^{4+})_2(O^{2-})_4$. Other authors conclude that these charge states are Mn^{2+} and Mn^{3+} for both phases, see for example Ref 20-23. Taking other manganese containing spinels into consideration, e.g. the Mn-Ni system, the model with Mn^{4+} ions is preferred. β-Spinel dissolve more nickel than $NiMn_2O_4$, thus β-spinel in Mn-Ni can not sufficiently be described without using Mn^{4+} ions on octahedral sites. In this work it is assumed that α- and β-Mn_3O_4 have different ionic configurations: stoichiometric α-Mn_3O_4 is described by $(Mn^{2+}, Mn^{3+})_1(Mn^{2+}, Mn^{3+})_2(O^{2-})_4$ and β-Mn_3O_4 by $(Mn^{2+})_1(Mn^{2+}, Mn^{3+}, Mn^{4+})_2(O^{2-})_4$.

3. Cubic Hausmannite (β-Mn_3O_4)

The complete description of the spinel phase is rather complicated why a stoichiometric spinel is considered as a first approach, which is modelled using the formula $(Mn^{2+})_1(Mn^{2+}, Mn^{3+}, Mn^{4+})_2(O^{2-})_4$. The first sublattice represents tetrahedral sites and the second sublattice represents octahedral sites. A normal spinel has the trivalent ions on the octahedral sites and the divalent ions on the tetrahedral sites. If the octahedral sites are occupied by divalent and tetravalent ions the spinel is referred to as inverse. The three ${}^{o}G$ parameters $\left({}^{o}G^{\beta}_{Mn^{2+}:Mn^{2+}},\ {}^{o}G^{\beta}_{Mn^{2+}:Mn^{3+}}, \text{ and } {}^{o}G^{\beta}_{Mn^{2+}:Mn^{4+}}\right)$ are from now on denoted ${}^{o}G^{\beta}_{22}$, ${}^{o}G^{\beta}_{23}$, and ${}^{o}G^{\beta}_{24}$. The Gibbs energy of stoichiometric β-Mn_3O_4 is given by

$$
{}^{o}G^{\beta}_{m} = y'_2y''_2{}^{o}G^{\beta}_{22} + y'_2y''_3{}^{o}G^{\beta}_{23} + y'_2y''_4{}^{o}G^{\beta}_{24} - TS_m + {}^{E}G_m \qquad \text{(Eq 3)}
$$

where the superscripts $'$ and $''$ denote tetrahedral and octahedral sites, respectively. This is a system with a neutral line between the ${}^{o}G^{\beta}_{23}$ corner and the middle of the ${}^{o}G^{\beta}_{22} - {}^{o}G^{\beta}_{24}$ side. All points on the neutral line between the normal and inverse spinels represent the stoichiometric composition, but with different distributions of ions on the octahedral sublattice. Only one point on the line represents the equilibrium composition at a given temperature. Only two parameters can normally be evaluated since there are two pieces of information, the Gibbs energy of the equilibrium phase and the degree of inversion. The site fractions in Eq 3 are replaced by a variable describing the disorder, ξ. $\xi = 0$ yields the normal state $(Mn^{2+})_1(Mn^{3+})_2$ and $\xi = 1$ yields the inverse state $(Mn^{2+})_1(Mn^{2+}_{0.5}, Mn^{4+}_{0.5})_2$. ξ is an expression of the degree of inversion and can be used to express all site fractions, $\xi = 1 - y''_3 = 2y''_2 = 2y''_4$, $y'_2 = 1$. All interaction energies in Eq 3 should be neglected since there already are more compound energies than experimental information, i.e. ${}^{E}G_m$ is set to zero. Rearranging Eq 3 and expressing all site fractions in terms of ξ yields:

$$
G^{\beta}_{m} + TS_m(\xi) = {}^{o}G^{\beta}_{23} + J^{\beta}_{234}\xi \qquad \text{(Eq 4)}
$$

$$
J^{\beta}_{234} = 0.5{}^{o}G^{\beta}_{22} + 0.5{}^{o}G^{\beta}_{24} - {}^{o}G^{\beta}_{23} \qquad \text{(Eq 5)}
$$

Gibbs energy of β-Mn_3O_4 is given by the parameter ${}^{o}G^{\beta}_{33}$ and J^{β}_{234} is used to model the degree of inversion. ${}^{o}G^{\beta}_{22}$ is used as a reference and can adopt any value. If Mn-O was assessed without the intention to include the description in a larger system the easiest choice would be to put ${}^{o}G^{\beta}_{22} = 0$. But since a reference already is chosen in Fe_3O_4, ${}^{o}G^{\beta}_{22}$ will adopt a value from the Fe-Mn-O assessment that is compatible with the reference in Fe-O. This gives the following parameters for stoichiometric β-Mn_3O_4:

$${}^{o}G^{\beta}_{22} \quad \text{reference} \qquad \text{(Eq 6)}$$

$${}^{o}G^{\beta}_{23} = 7G^{\beta}_{Mn_3O_4} \qquad \text{(Eq 7)}$$

$${}^{o}G^{\beta}_{24} = 14G^{\beta}_{Mn_3O_4} + J^{\beta}_{Mn_3O_4} - {}^{o}G^{\beta}_{22} \qquad \text{(Eq 8)}$$

β-Mn_3O_4 shows a small deviation from stoichiometry. Vacant sites are formed in the octahedral sublattice to maintain electroneutrality when excess Mn^{4+} is introduced to model the deviation towards oxygen in equilibrium with Mn_2O_3. The extended spinel model is then $\left(Mn^{2+}\right)_1\left(Mn^{2+}, Mn^{3+}, Mn^{4+}, Va\right)_2\left(O^{2-}\right)_4$. Several combinations to form neutral Mn_2O_3 with spinel structure are found in this formula. One of them is used to describe the deviation from stoichiometry towards oxygen. Gibbs energy of this Mn_2O_3 is

$${}^{o}G^{\beta}_{m} = \left(2{}^{o}G^{\beta}_{23} + 3{}^{o}G^{\beta}_{24} + {}^{o}G^{\beta}_{2V} - 2RT\left(6\ \ln(6) - 3\ \ln(3) - 2\ \ln(2)\right)\right)\Big/6 \qquad \text{(Eq 9)}$$

where ${}^{o}G^{\beta}_{2V}$ is used to describe the solubility of O in the spinel. To model deviation towards manganese in equilibrium with halite, Mn^{2+} is assumed to enter interstitial sites normally filled with vacancies. The final spinel model for β-Mn_3O_4 is $\left(Mn^{2+}\right)_1\left(Mn^{2+}, Mn^{3+}, Mn^{4+}, Va\right)_2\left(Mn^{2+}, Va\right)_2\left(O^{2-}\right)_4$. A new neutral endpoint is found, a hypothetical metastable MnO with spinel structure. Gibbs energy of this endpoint is

$${}^{o}G^{\beta}_{m} = \left({}^{o}G^{\beta}_{22V} + {}^{o}G^{\beta}_{222} - 4\ RT\ \ln(2)\right)\Big/2 \qquad \text{(Eq 10)}$$

where ${}^{o}G^{\beta}_{222}$ is used to describe the solubility of Mn in the spinel. The remaining three ${}^{o}G$ parameters $\left({}^{o}G^{\beta}_{232}, {}^{o}G^{\beta}_{242}, \text{ and } {}^{o}G^{\beta}_{2V2}\right)$ are obtained from reciprocal reactions ($\Delta G_{223:2V2}$, $\Delta G_{224:2V2}$, $\Delta G_{22V:2V2}$), where all reactions are assumed to have $\Delta G = 0$.

4. Tetragonal Hausmannite (α-Mn_3O_4)

The stoichiometric tetragonal spinel is modelled using the formula $\left(Mn^{2+}, Mn^{3+}\right)_1\left(Mn^{2+}, Mn^{3+}\right)_2\left(O^{2-}\right)_4$. The four ${}^{o}G$ parameters $\left({}^{o}G^{\alpha}_{Mn^{2+}:Mn^{2+}}, {}^{o}G^{\alpha}_{Mn^{2+}:Mn^{3+}}, {}^{o}G^{\alpha}_{Mn^{3+}:Mn^{2+}} \text{ and } {}^{o}G^{\alpha}_{Mn^{3+}:Mn^{3+}}\right)$ are from now on denoted ${}^{o}G^{\alpha}_{22}$, ${}^{o}G^{\alpha}_{23}$, ${}^{o}G^{\alpha}_{32}$ and ${}^{o}G^{\alpha}_{33}$. Gibbs energy of stoichiometric α-Mn_3O_4 is given by

$${}^{o}G^{\alpha}_{m} = y'_2y''_2{}^{o}G^{\alpha}_{22} + y'_2y''_3{}^{o}G^{\alpha}_{23} + y'_3y''_2{}^{o}G^{\alpha}_{32} + y'_3y''_3{}^{o}G^{\alpha}_{33} - TS_m + {}^{E}G_m \qquad \text{(Eq 11)}$$

This is a reciprocal system, with a neutral line between the ${}^{o}G^{\alpha}_{23}$ corner and the middle of the ${}^{o}G^{\alpha}_{32} - {}^{o}G^{\alpha}_{33}$ side. How to choose the optimizing parameters for a 23-spinel is discussed in detail by Hillert et al.[24] The site fractions in Eq 11 are replaced by a variable describing the disorder, ξ. ξ = 0 yields the normal state $\left(Mn^{2+}\right)_1\left(Mn^{3+}\right)_2$ and ξ = 1 yields the inverse state $\left(Mn^{3+}\right)_1\left(Mn^{2+}_{0.5}, Mn^{3+}_{0.5}\right)_2$. α-$Mn_3O_4$ is a normal spinel with low degree of inversion. ξ is an expression of the degree of inversion and can be used to express all site fractions, $\xi = y'_3 = 1 - y'_2 = 2y''_2 = 2\left(1 - y''_3\right)$. Rearranging Eq 11, neglecting all interaction energies and expressing all site fractions in terms of ξ yields:

$$G^{\alpha}_{m} + TS_m(\xi) = {}^{o}G^{\alpha}_{23} + 0.5J^{\alpha}_{23}\xi + 0.5\Delta G_{23:23}\xi^2 \qquad \text{(Eq 12)}$$

$$J^{\alpha}_{23} = {}^{o}G^{\alpha}_{22} - 3{}^{o}G^{\alpha}_{23} + 2{}^{o}G^{\alpha}_{33} \qquad \text{(Eq 13)}$$

$$\Delta G_{23:23} = {}^{o}G^{\alpha}_{23} + {}^{o}G^{\alpha}_{32} - {}^{o}G^{\alpha}_{22} - {}^{o}G^{\alpha}_{33} \qquad \text{(Eq 14)}$$

Gibbs energy of α-Mn_3O_4 is given by the parameter ${}^{o}G^{\alpha}_{23}$ and J^{α}_{23} is used to model the degree of inversion. ${}^{o}G^{\alpha}_{33}$ is used as a reference and will adopt a value from the Fe-Mn-O assessment that is compatible with the reference in the Fe-O assessment. The last parameter, ${}^{o}G^{\alpha}_{32}$, is determined by the reciprocal reaction, where $\Delta G_{23:23} = 0$ is chosen. This gives the following parameters for stoichiometric α-Mn_3O_4:

$${}^{o}G^{\alpha}_{22} = 21G^{\alpha}_{Mn_3O_4} + 2J^{\alpha}_{Mn_3O_4} - 2{}^{o}G^{\alpha}_{33} \qquad \text{(Eq 15)}$$

$${}^{o}G^{\alpha}_{23} = 7G^{\alpha}_{Mn_3O_4} \qquad \text{(Eq 16)}$$

$${}^{o}G^{\alpha}_{32} = 14G^{\alpha}_{Mn_3O_4} + 2J^{\alpha}_{Mn_3O_4} - {}^{o}G^{\alpha}_{33} \qquad \text{(Eq 17)}$$

$${}^{o}G^{\alpha}_{33} \quad \text{reference} \qquad \text{(Eq 18)}$$

In the same way as β-Mn_3O_4, α-Mn_3O_4 also shows a small deviation from stoichiometry. The complete model is $\left(Mn^{2+}, Mn^{3+}\right)_1\left(Mn^{2+}, Mn^{3+}, Va\right)_2\left(Mn^{2+}, Va\right)_2\left(O^{2-}\right)_4$.

Two new neutral endpoints are found, hypothetical metastable Mn_2O_3 and MnO with spinel structure. The Gibbs energy of these endpoints are

$${}^{o}G^{\alpha}_{m} = \left(5{}^{o}G^{\alpha}_{33V} + {}^{o}G^{\alpha}_{3VV} - 2RT(6\ \ln(6) - 5\ \ln(5))\right)/6 \qquad \text{(Eq 19)}$$

$${}^{o}G^{\alpha}_{m} = \left({}^{o}G^{\alpha}_{22V} + {}^{o}G^{\alpha}_{222} - 4\ RT\ \ln(2)\right)/2 \qquad \text{(Eq 20)}$$

where ${}^{o}G^{\alpha}_{3VV}$ and ${}^{o}G^{\alpha}_{222}$ are used to describe the solubility of O and Mn respectively in α-spinel. The remaining ${}^{o}G$ parameters $\left({}^{o}G^{\alpha}_{2VV}, {}^{o}G^{\alpha}_{232}, {}^{o}G^{\alpha}_{2V2}, {}^{o}G^{\alpha}_{322}, {}^{o}G^{\alpha}_{332}, {}^{o}G^{\alpha}_{3V2}\right)$ are obtained from reciprocal reactions, where all reactions are assumed to have $\Delta G = 0$.

The high temperature β-Mn_3O_4 is modelled relative to α-Mn_3O_4 by:

$$^{o}G^{\alpha}_{23V} = {}^{o}G^{\beta}_{23V} + A + BT \quad \text{(Eq 21)}$$

5. Cubic Fe-Mn Spinel

The complete cubic Fe-Mn spinel, which besides magnetite and hausmannite consists of jacobsite ($MnFe_2O_4$), is thus modelled as:

$$\left(Fe^{2+}, Fe^{3+}, Mn^{2+}\right)_1\left(Fe^{2+}, Fe^{3+}, Mn^{2+}, Mn^{3+}, Mn^{4+}, Va\right)_2 \left(Fe^{2+}, Mn^{2+}, Va\right)_2\left(O^{2-}\right)_4$$

The subsystem used to model stoichiometric jacobsite is $\left(Fe^{3+}, Mn^{2+}\right)_1\left(Fe^{3+}, Mn^{2+}\right)_2\left(O^{2-}\right)_4$. This reciprocal system will generate equivalent expressions as in Eq 12-14. As in the model for stoichiometric α-Mn_3O_4, two parameters can be obtained from experiments: Gibbs energy of $MnFe_2O_4$ and the degree of inversion. ${}^{o}G^{\beta}_{Mn^{2+}:Fe^{3+}}$ is used to model the Gibbs energy of jacobsite $\left(G^{\beta}_{MnFe_2O_4}\right)$, ${}^{o}G^{\beta}_{Fe^{3+}:Mn^{2+}}$ the degree of inversion $\left(J^{\beta}_{MnFe_2O_4}\right)$ and ${}^{o}G^{\beta}_{Fe^{3+}:Fe^{3+}}$ is already fixed from the Fe-O assessment. The reciprocal reaction, $\Delta G_{Mn^{2+},Fe^{3+}:Mn^{2+},Fe^{3+}} = 0$ will give us the ${}^{o}G^{\beta}_{Mn^{2+}:Mn^{2+}}$ parameter which is used in the model for Mn_3O_4. This gives the following parameters for stoichiometric $MnFe_2O_4$:

$$^{o}G^{\beta}_{Mn^{2+}:Mn^{2+}} = 21G^{\beta}_{MnFe_2O_4} + 2J^{\beta}_{MnFe_2O_4} - 14G^{\beta}_{Fe_3O_4} + 2B^{\beta}_{Fe_3O_4} \quad \text{(Eq 22)}$$

$$^{o}G^{\beta}_{Mn^{2+}:Fe^{3+}} = 7G^{\beta}_{MnFe_2O_4} \quad \text{(Eq 23)}$$

$$^{o}G^{\beta}_{Fe^{3+}:Mn^{2+}} = 7G^{\beta}_{Fe_3O_4} - B^{\beta}_{Fe_3O_4} - 7G^{\beta}_{MnFe_2O_4} + {}^{o}G^{\beta}_{Mn^{2+}:Mn^{2+}} \quad \text{(Eq 24)}$$

$$^{o}G^{\beta}_{Fe^{3+}:Fe^{3+}} = 7G^{\beta}_{Fe_3O_4} - B^{\beta}_{Fe_3O_4} \quad \text{(Eq 25)}$$

It may seem strange that the ${}^{o}G^{\beta}_{Mn^{2+}:Mn^{2+}}$ compound involve parameters evaluated in the assessment of both Fe_3O_4 and $MnFe_2O_4$ although it does not contain any Fe. This arises because there could only be one ${}^{o}G$ parameter acting as reference in a phase and the reference in the spinel phase is agreed to be ${}^{o}G^{\beta}_{Fe^{2+}:Fe^{3+}} = {}^{o}G^{\beta}_{Fe^{3+}:Fe^{2+}}$. It would be possible to choose another reference, i.e. ${}^{o}G^{\beta}_{Mn^{2+}:Mn^{2+}} = 0$, and adjust the Fe_3O_4 and the $MnFe_2O_4$ values accordingly. This would give different values on all ${}^{o}G$ parameters that have a net charge, but the description would be identical.

There are still six parameters in the Fe-Mn system needed to be fixed in a proper way $\left({}^{o}G^{\beta}_{Fe^{2+}:Mn^{2+}}, {}^{o}G^{\beta}_{Fe^{2+}:Mn^{3+}}, {}^{o}G^{\beta}_{Fe^{2+}:Mn^{4+}}, {}^{o}G^{\beta}_{Fe^{3+}:Mn^{3+}}, {}^{o}G^{\beta}_{Fe^{3+}:Mn^{4+}}\right.$ and $\left.{}^{o}G^{\beta}_{Mn^{2+}:Fe^{2+}}\right)$. Some of these parameters could be obtained by setting reciprocal reactions equals zero, while others need to be evaluated using some other expressions. Another subsystem in stoichiometric Fe-Mn spinel is $\left(Fe^{2+}, Mn^{2+}\right)_1\left(Fe^{2+}, Mn^{3+}, Mn^{4+}\right)_2\left(O^{2-}\right)_4$, which can be used to model one more possible neutral spinel, $FeMn_2O_4$. Gibbs energy of this subsystem is given by

$$G^{\beta}_{m} + TS_m(\xi) = {}^{o}G^{\beta}_{Fe^{2+}:Mn^{3+}} + J^{\beta}_{FeMn_2O_4}\xi + D^{\beta}_{FeMn_2O_4}\xi^2 \quad \text{(Eq 26)}$$

$$J^{\beta}_{FeMn_2O_4} = 0.5{}^{o}G^{\beta}_{Fe^{2+}:Fe^{2+}} + 0.5{}^{o}G^{\beta}_{Fe^{2+}:Mn^{4+}} - 2{}^{o}G^{\beta}_{Fe^{2+}:Mn^{3+}} + G^{\beta}_{Mn^{2+}:Mn^{3+}} \quad \text{(Eq 27)}$$

$$D^{\beta}_{FeMn_2O_4} = -0.5{}^{o}G^{\beta}_{Fe^{2+}:Fe^{2+}} - 0.5{}^{o}G^{\beta}_{Fe^{2+}:Mn^{4+}} + {}^{o}G^{\beta}_{Fe^{2+}:Mn^{3+}} + 0.5{}^{o}G^{\beta}_{Mn^{2+}:Fe^{2+}} + 0.5{}^{o}G^{\beta}_{Mn^{2+}:Mn^{4+}} - {}^{o}G^{\beta}_{Mn^{2+}:Mn^{3+}} \quad \text{(Eq 28)}$$

where ξ is the degree of inversion. This is a system with a neutral line between the ${}^{o}G^{\beta}_{Fe^{2+}:Mn^{3+}}$ corner and the ${}^{o}G^{\beta}_{Mn^{2+}:Fe^{2+}} - {}^{o}G^{\beta}_{Mn^{2+}:Mn^{4+}}$ side. If $D^{\beta}_{FeMn_2O_4}$ is assumed to be equal to zero, Eq 27 will reduce to

$$J^{\beta}_{FeMn_2O_4} = 0.5{}^{o}G^{\beta}_{Mn^{2+}:Fe^{2+}} + 0.5{}^{o}G^{\beta}_{Mn^{2+}:Mn^{4+}} - {}^{o}G^{\beta}_{Fe^{2+}:Mn^{3+}} \quad \text{(Eq 29)}$$

which is rather obvious the parameter describing the degree of inversion of $FeMn_2O_4$. The Gibbs energy of $FeMn_2O_4$ is given by the parameter ${}^{o}G^{\beta}_{Fe^{2+}:Mn^{3+}}$ and the third parameter, ${}^{o}G^{\beta}_{Fe^{2+}:Mn^{4+}}$, is given by Eq 28.

The remaining three ${}^{o}G$ parameters in the stoichiometric system $\left({}^{o}G^{\beta}_{Fe^{2+}:Mn^{2+}}, {}^{o}G^{\beta}_{Fe^{3+}:Mn^{3+}}\right.$ and $\left.{}^{o}G^{\beta}_{Fe^{3+}:Mn^{4+}}\right)$ are related to the previously mentioned parameters by reciprocal reactions ($\Delta G_{Fe^{2+},Mn^{2+}:Fe^{3+},Mn^{2+}} = \Delta G_{Fe^{3+},Mn^{2+}:Fe^{3+},Mn^{3+}} = \Delta G_{Fe^{3+},Mn^{2+}:Mn^{2+},Mn^{4+}} = 0$. For the nonstoichiometric system, all 26 parameters are evaluated using $\Delta G = 0$.

6. Tetragonal Fe-Mn Spinel

Fe has a low solubility in the tetragonal α-spinel, but to be able to correctly model the tetragonal phase, it is in this assessment described all the way to the metastable α-Fe_3O_4. It makes very little difference what values are chosen for the majority of those parameters. We choose, rather arbitrarily, the same functions for many parameters in the tetragonal spinel as we did in the cubic spinel.

6.1 Wustite, Manganosite, Hematite, β-Bixbyite and Pyrolusite

The wustite ($Fe_{1-x}O$) and manganosite ($Mn_{1-x}O$) phases are isomorphous both having the NaCl-type structure

(Strukturbericht B1), with generic name halite. The halite phase is described using a model within the CEF with two sublattices; one for metal ions and one for oxygen. Both $Fe_{1-x}O$ and $Mn_{1-x}O$ have a considerable solid solubility, due to the oxidation of Fe^{2+} to Fe^{3+} and Mn^{2+} to Mn^{3+} respectively and the formation of cation vacancies. The phase is thus represented as:

$$\left(Fe^{2+}, Fe^{3+}, Mn^{2+}, Mn^{3+}, Va\right)_1\left(O^{2-}\right)_1$$

Hematite (Fe_2O_3) with the generic name corundum (Strukturbericht $D5_1$) is described with a small deviation from stoichiometry with a model within the CEF using three sublattices. The solubility of Mn in hematite is modelled by adding Mn^{3+} ions on the first sublattice. The phase is thus represented as:

$$\left(Fe^{2+}, Fe^{3+}, Mn^{3+}\right)_2\left(Fe^{3+}, Va\right)_1\left(O^{2-}\right)_3$$

The end member Mn^{3+}:Va:O^{2-} is used to model the solubility of Mn in hematite. Mn^{3+}:Fe^{3+}:O^{2-} is derived using the reciprocal reaction:

$${}^{o}G_{Mn^{3+}:Fe^{3+}} - {}^{o}G_{Mn^{3+}:Va} = {}^{o}G_{Fe^{3+}:Fe^{3+}} - {}^{o}G_{Fe^{3+}:Va}$$

α-Bixbyite (α-Mn_2O_3) transforms to β-Mn_2O_3 (Strukturbericht $D5_3$) at around 300 K. The α-modification was not considered due to the low transformation temperature. The solubility of Fe in β-bixbyite is modelled by adding Fe^{3+} ions on the cation sublattice. The phase is thus represented as:

$$\left(Fe^{3+}, Mn^{3+}\right)_2\left(O^{2-}\right)_3$$

Pyrolusite (MnO_2) with the generic name rutile (Strukturbericht C4) is described as a stoichiometric phase. There are no reports on solubility of Fe in pyrolusite.

The description of $Fe_{1-x}O$ is taken from Sundman[8] and the description of Fe_2O_3 is from Kjellqvist et al.[1] The descriptions for $Mn_{1-x}O$, β-Mn_2O_3 and MnO_2 are all from Grundy et al.[11]

7. Experimental Data

7.1 Mn_3O_4

With increasing temperature, Mn_3O_4 transforms from tetragonal α-Mn_3O_4 to cubic β-Mn_3O_4. The measured temperatures at which this transformation takes place varies between 1403 and 1473 K in air at 1 atmosphere total pressure, with a larger group between 1443 and 1450 K.[20,25-34] The transformation enthalpy has been measured by three authors ranging from 18 to 22.82 kJ/mole.[26-28] The nonstoichiometry of hausmannite has been investigated by a number of authors, some of them find it to be stoichiometric Mn_3O_4,[35-39] while others find different degree of nonstoichiometry.[20,30,31,40-46] β-Mn_3O_4 melts according to β-Mn_3O_4 → liquid + gas. The measured temperatures ranging from 1835 to 1863 K.[32,33,36,42,47] The eutectic between liquid β-Mn_3O_4 and halite[33,35,36,42] and the reaction Mn_2O_3 → β-Mn_3O_4 + gas[25,34,36,39,48-52] have also been measured numerous times.

Table 1 Thermodynamic data of Mn_3O_4

	Reference
$\Delta_f^o H_{298}$, kJ/mol	
1373.27	Le Chatelier and Daubrée[53]
1377.46	Ruff and Gersten[54]
1444.45	Roth[55]
1408.86	Siemonsen[56]
1408.44	Ulich and Siemonsen[57]
1388.55	Shomate[38]
1387.09	Mah,[58] Zordan and Hepler[59]
1387.51	Robie and Waldbaum[60]
1388.78	Pankratz[25]
1386.1	Knacke et al.[61]
1387.4	Kubaschewski et al.[62]
1382.74	Grundy et al.[11]
1385.40	This work
${}^{o}S_{298}$, J/mole, K	
155.75	Pankratz[25]
166.6	O'Neill and Pownceby[63]
149.59	Millar[37]
164.1	Robie and Hemingway[64]
167.1	Chhor et al.[65]
154.8	Kubaschewski et al.[62]
154.07	Zordan and Hepler[59]
168.34	Grundy et al.[11]
165.71	This work
$\Delta H^{\alpha\rightarrow\beta}$, kJ/mol	
18	Southard and Moore[28]
20.9	Irani et al.[27]
22.82	Ramano Rao and Tare[26]
18.13	Pankratz[25]
20.8	Grundy et al.[11]
21.01	This work

There are many determinations on the enthalpy of formation, $\Delta_f^o H_{298}$,[25,38,53-62] the entropy at 298.15 K, ${}^{o}S_{298}$,[25,37,59,62-65] and heat capacity, c_p,[37,64,65] see Table 1. The heat content of α-Mn_3O_4 has been measured by Southard and Moore[28] and Fritsch and Navrotsky.[66] The magnetic transition temperature was measured by two authors[64,65] with excellent agreement between their values, 43.15 and 43.12 K respectively.

The non-configurational free energy change on converting a normal to an inverse α-spinel ($\Delta G_D = G_i - G_n + TS_m = 0.5J_{23}^{\alpha}$) has been calculated from crystal field theory by several authors.[21,22,67] Dorris and Mason[19] measured the ionic configuration for β-Mn_3O_4.

7.2 Fe-Mn-O

The nonstoichiometry of $(Fe_{1-x}Mn_x)_{1-\delta}O$ has been investigated at different temperatures and compositions.[68-72] There are a number of investigations on the two-phase region between halite and fcc[52,68,69,72-77] and halite and spinel.[52,68,69,72,74-80] Ref 52, 69, 73, 77, 81-83 measured the activity of FeO at the two-phase equilibrium fcc/halite.

The phase relations in the system Fe_2O_3-Mn_2O_3 have been examined by several authors.[75,84-88] Bixbyite has large solubility of iron, approximately 70% at the peritectoid reaction between bixbyite, corundum and β-spinel in air, while the solubility of Mn in corundum at the same reaction is approximately 13%.

The two-phase region between corundum and spinel at 1273 K has been investigated by Ref 69, 75, 76.

Fe_3O_4 and β-Mn_3O_4 forms a continuous solid solution down to 1443 K at the manganese side, where β-Mn_3O_4 transforms to α-Mn_3O_4. While β-Mn_3O_4 is isomorph with Fe_3O_4, α-Mn_3O_4 has a limited solubility of iron. The miscibility limits of the α-Mn_3O_4/β-Mn_3O_4 transformation has been determined by Ref 32, 79, 86, 89-92. Jacobsite ($MnFe_2O_4$) is a normal spinel at low temperatures, with an increasing degree of inversion at higher temperatures. The cation distribution of jacobsite has been studied by several authors.[93-99] The oxygen nonstoichiometry of β-spinel has been measured by Bulgakova and Rozanov[74] and Terayama et al.[100]

The enthalpy of formation, $\Delta_f^o H_{298}$, and the entropy at 298.15 K, ${}^oS_{298}$, for $MnFe_2O_4$ are tabulated by Kubaschewski et al.[62] Heat content, $H\text{-}H_{298}$, and heat capacity, c_p, for temperatures ranging from 298 to 1000 K have been measured by Reznitskii.[101] Naito et al.[102] measured c_p for the spinels $MnFe_2O_4$, $Mn_{1.5}Fe_{1.5}O_4$ and Mn_2FeO_4 between 200 and 740 K. Curie temperatures in Fe_3O_4-Mn_3O_4 at different compositions are determined with good agreement between the authors.[101-106]

Nölle[107] measured the phase boundary between liquid oxide and halite at 1823 K. The phase boundary between liquid oxide and spinel has been measured by Muan and Somiya.[84] A number of studies report the solubility of oxygen in liquid Fe-Mn alloys at 1873 K,[52,84,108-114] with a wide scatter in the different data.

8. Optimization and Results

The optimization of the parameters was performed using the PARROT module of the Thermo-Calc software.[115] The values for the interaction parameters assessed in this work are listed in Table 2. Data for the pure elements were taken from Dinsdale.[116]

8.1 Mn-O

The descriptions of all phases in Mn-O from Grundy et al.[11] except the liquid, α- and β-Mn_3O_4 are unchanged. The calculated phase diagram is shown in Fig. 1.

α-Mn_3O_4 is known to be a normal spinel[19,20,117] with Mn^{2+} occupying the tetrahedral sites and Mn^{3+} occupying the octahedral sites. Some interchange between the sites will however occur. The calculated stabilization energies from Dunitz and Orgel[22] were used to evaluate a parameter to describe the cation distribution between tetrahedral and octahedral sites. The cation distribution for β-Mn_3O_4 is consistent with experiments from Dorris and Mason.[19]

The investigation on the nonstoichiometry of α- and β-Mn_3O_4 from Keller and Dieckmann[30] was then used to evaluate the two parameters in each phase describing the deviation from stoichiometry towards lower and higher oxygen contents by formation of cation interstitials and octahedral vacancies. The assessed heat capacity from Grundy et al.[11] was kept, but the enthalpy of formation and entropy at 298.15 K needed to be adjusted in order to fit the nonstoichiometry data, the enthalpy of the α-Mn_3O_4/β-Mn_3O_4 transformation and the transition temperature. The enthalpy of formation, the entropy at 298.15 K and the enthalpy of the α-Mn_3O_4/β-Mn_3O_4 transformation from literature are compared to this assessment in Table 1. The magnetic transition temperature was fixed to the experimental value of 43.15 K measured by Chhor et al.[65]

In Fig. 2 the enthalpy of α-Mn_3O_4 is plotted against experimental data. The calculated oxygen potential inside the two spinel phases is shown in Fig. 3 and 4.

The liquid parameters for the Mn-O system using the $MnO_{1.5}$ species instead of the Mn^{3+} species, are obtained from the previous description without any reassessment using

$${}^oG_{MnO_{1.5}} = 0.5\,{}^oG_{Mn^{3+}:O^{2-}} \quad \text{(Eq 30)}$$

$$L_{Mn^{2+}:O^{2-},MnO_{1.5}} = L_{Mn^{2+},Mn^{3+}:O^{2-}} \quad \text{(Eq 31)}$$

Equivalent to the Fe-O system, an additional parameter, $L_{Mn^{2+}:Va^{Q-},MnO_{1.5}}$, was introduced and optimized to obtain an almost identical fit to the phase diagram as the previous model using Mn^{3+}.

8.2 Fe-Mn-O

Data for the Fe-Mn and Fe-O systems were taken from existing assessments from Huang[12] and Sundman[8] (modified by Selleby and Sundman,[9] Kowalski and Spencer,[10] Kjellqvist et al.[1]) respectively.

When optimizing the cubic spinel phase, the parameter ${}^oG_{Mn^{2+}:Fe^{3+}}$ is first determined against the enthalpy of formation, $\Delta_f^o H_{298}$,[62] the entropy at 298.15 K, ${}^oS_{298}$,[62] heat content, $H\text{-}H_{298}$,[100] and heat capacity, c_p,[100] for $MnFe_2O_4$. The magnetic transition temperature was fixed to the experimental value of 577 K, and the Bohr magneton number, ${}^0\beta$, was used as the optimizing parameter to fit the λ-peak in the heat capacity curve. The enthalpy and heat capacity together with experimental data is shown in Fig. 5 and 6.

Curie temperatures for Fe-Mn-O spinels have been measured and an excess parameter for the Curie temperature between Mn_3O_4 and $MnFe_2O_4$ is needed to reproduce the correct behavior. The calculated and experimental Curie temperature between Fe_3O_4 and Mn_3O_4 is shown in Fig. 7.

Tetragonal $MnFe_2O_4$ is not stable at normal conditions and the parameter ${}^oG^{\alpha}_{Mn^{2+}:Fe^{3+}}$ is used to reproduce the solubility limit of Fe in tetragonal spinel. The calculated phase diagram Fe_3O_4-Mn_3O_4 is shown in Fig. 7.

The distribution of cations between tetrahedral and octahedral sites in $MnFe_2O_4$ has been studied by a number of authors, with different results. Jirák and Vratislav[97] did

Table 2 Assessed parameters (in SI units: J, mole, K)

The magnetic contribution to Gibbs energy is described by:

$G^{magn} = RT\ln(\beta + 1)f(\tau)$, $\tau = T/T_C$

For $\tau < 1$:

$f(\tau) = 1 - [79\tau^{-1}/140p + 474/497(1/p - 1)(\tau^3/6 + \tau^9/135 + \tau^{15}/600)]/A$

and for $\tau > 1$:

$f(\tau) = -(\tau^{-5}/10 + \tau^{-15}/315 + \tau^{-25}/1600)/A$

where $A = 518/1125 + 11692/15975(1/p - 1)$ and p depends on the structure

Liquid $\left(\mathbf{Fe^{2+}}, \mathbf{Mn^{2+}}\right)_P \left(\mathbf{O^{2-}}, \mathbf{Va}^{Q-}, \mathbf{FeO_{1.5}}, \mathbf{MnO_{1.5}}\right)_Q$

$^{o}G_{Fe^{2+}:O^{2-}} - H^{SER}_{Fe} - 2H^{SER}_{O} = 4GFEOLIQ$

$^{o}G_{Fe^{2+}:Va} - H^{SER}_{Fe} = GFELIQ$

$^{o}G_{FeO_{1.5}} - H^{SER}_{Fe} - 1.5H^{SER}_{O} = 2.5GFEOLIQ - 89819 + 39.962T$

$^{o}G_{Mn^{2+}:O^{2-}} - 2H^{SER}_{Mn} - 2H^{SER}_{O} = 2GMN1O1\_L$

$^{o}G_{Mn^{2+}:Va} - H^{SER}_{Mn} = GMN\_L$

$^{o}G_{MnO_{1.5}} - H^{SER}_{Mn} - 1.5H^{SER}_{O} = 0.5GMN2O3\_L$

$^{0}L_{Fe^{2+}:O^{2-},Va} = 176681 - 16.368T$

$^{1}L_{Fe^{2+}:O^{2-},Va} = -65655 + 30.869T$

$^{0}L_{Fe^{2+}:O^{2-},FeO_{1.5}} = -26362$

$^{1}L_{Fe^{2+}:O^{2-},FeO_{1.5}} = 13353$

$^{0}L_{Fe^{2+}:Va,FeO_{1.5}} = 110000$

$^{0}L_{Mn^{2+}:O^{2-},Va} = 129519$

$^{1}L_{Mn^{2+}:O^{2-},Va} = -45459$

$^{0}L_{Mn^{2+}:O^{2-},MnO_{1.5}} = -33859$

$^{0}L_{Mn^{2+}:Va,MnO_{1.5}} = 110000^{*}$

$^{0}L_{Fe^{2+},Mn^{2+}:Va} = -3950 + 0.489T$

$^{1}L_{Fe^{2+},Mn^{2+}:Va} = 1145$

$^{0}L_{Fe^{2+},Mn^{2+}:O^{2-}} = -11000^{*}$

$^{1}L_{Fe^{2+},Mn^{2+}:O^{2-}} = -4700^{*}$

$^{0}L_{Fe^{2+}:Va,MnO_{1.5}} = 110000^{*}$

$^{0}L_{Mn^{2+}:Va,FeO_{1.5}} = 110000^{*}$

$^{0}L_{Mn^{2+}:O^{2-},FeO_{1.5}} = -47000^{*}$

Halite: $\left(\mathbf{Fe^{2+}}, \mathbf{Fe^{3+}}, \mathbf{Mn^{2+}}, \mathbf{Mn^{3+}}, \mathbf{Va}\right)_1 \left(\mathbf{O^{2-}}\right)_1$

$^{o}G_{Fe^{2+}:O^{2-}} - H^{SER}_{Fe} - H^{SER}_{O} = GWUSTITE$

$^{o}G_{Fe^{3+}:O^{2-}} - H^{SER}_{Fe} - H^{SER}_{O} = 1.25AWUSTITE + 1.25GWUSTITE$

$^{o}G_{Mn^{2+}:O^{2-}} - H^{SER}_{Mn} - H^{SER}_{O} = GMN1O1$

$^{o}G_{Mn^{3+}:O^{2-}} - H^{SER}_{Mn} - H^{SER}_{O} = GMN1O1 - 21884 - 22.185T$

$^{o}G_{Va:O^{2-}} - H^{SER}_{O} = 0$

$^{0}L_{Fe^{2+},Fe^{3+}:O^{2-}} = -12324.4$

$^{1}L_{Fe^{2+},Fe^{3+}:O^{2-}} = 20070$

$^{0}L_{Mn^{2+},Mn^{3+}:O^{2-}} = -42105$

$^{1}L_{Mn^{2+},Mn^{3+}:O^{2-}} = 46513$

$^{0}L_{Fe^{2+},Mn^{2+}:O^{2-}} = -1300^{*}$

$^{0}L_{Fe^{3+},Mn^{2+}:O^{2-}} = 11000^{*}$

$^{1}L_{Fe^{3+},Mn^{2+}:O^{2-}} = -28000^{*}$

$^{0}L_{Fe^{3+},Mn^{3+}:O^{2-}} = -23000 + 33T^{*}$

Corundum: $\left(\mathbf{Fe^{2+}}, \mathbf{Fe^{3+}}, \mathbf{Mn^{3+}}\right)_2 \left(\mathbf{Fe^{3+}}, \mathbf{Va}\right)_1 \left(\mathbf{O^{2-}}\right)_3$

$^{o}G_{Fe^{2+}:Fe^{3+}:O^{2-}} - 3H^{SER}_{Fe} - 3H^{SER}_{O} = GFE2O3 + 85000$

$^{o}G_{Fe^{3+}:Fe^{3+}:O^{2-}} - 3H^{SER}_{Fe} - 3H^{SER}_{O} = GFE2O3 + 85000$

$^{o}G_{Fe^{2+}:Va:O^{2-}} - 2H^{SER}_{Fe} - 3H^{SER}_{O} = GFE2O3$

$^{o}G_{Fe^{3+}:Va:O^{2-}} - 2H^{SER}_{Fe} - 3H^{SER}_{O} = GFE2O3$

$^{o}G_{Mn^{3+}:Fe^{3+}:O^{2-}} - 2H^{SER}_{Mn} - H^{SER}_{Fe} - 3H^{SER}_{O} = GMN2O3 + 110500 - 3.7T^{*}$

$^{o}G_{Mn^{3+}:Va:O^{2-}} - 2H^{SER}_{Mn} - 3H^{SER}_{O} = GMN2O3 + 25500 - 3.7T^{*}$

Table 2 continued

Magnetic properties (p = 0.28):
for compounds containing Fe cations on the first sublattice $T_C = -2867$ and $\beta = -25.1$
for compounds containing Mn cations on the first sublattice $T_C = 0$ and $\beta = 0$

Bixbyite: $(\mathbf{Fe^{3+}}, \mathbf{Mn^{3+}})_2(\mathbf{O^{2-}})_3$

${}^oG_{Fe^{3+}:O^{2-}} - 2H_{Fe}^{SER} - 3H_O^{SER} = GFE2O3 + 18000 - 10T^*$
${}^oG_{Mn^{3+}:O^{2-}} - 2H_{Mn}^{SER} - 3H_O^{SER} = GMN2O3$
${}^0L_{Fe^{3+},Mn^{3+}:O^{2-}} = 1500^*$

Pyrolusite: $(\mathbf{MnO_2})$: $(\mathbf{Mn^{4+}})_1(\mathbf{O^{2-}})_2$

${}^oG_{Mn^{4+}:O^{2-}} - H_{Mn}^{SER} - 2H_O^{SER} = -545091 + 395.379T - 65.277T\ln(T) - 0.007803T^2 + 664955/T$
$-0.007803T^2 + 664955/T$

β-Spinel: $(\mathbf{Fe^{2+}}, \mathbf{Fe^{3+}}, \mathbf{Mn^{2+}})_1(\mathbf{Fe^{2+}}, \mathbf{Fe^{3+}}, \mathbf{Mn^{2+}}, \mathbf{Mn^{3+}}, \mathbf{Mn^{4+}}, \mathbf{Va})_2(\mathbf{Fe^{2+}}, \mathbf{Mn^{2+}}, \mathbf{Va})_2(\mathbf{O^{2-}})_4$

${}^oG_{Fe^{2+}:Fe^{2+}:Va:O^{2-}} - 3H_{Fe}^{SER} - 4H_O^{SER} = 7GFFB + JFF$
${}^oG_{Fe^{3+}:Fe^{2+}:Va:O^{2-}} - 3H_{Fe}^{SER} - 4H_O^{SER} = 7GFFB$
${}^oG_{Fe^{2+}:Fe^{3+}:Va:O^{2-}} - 3H_{Fe}^{SER} - 4H_O^{SER} = 7GFFB$
${}^oG_{Fe^{3+}:Fe^{3+}:Va:O^{2-}} - 3H_{Fe}^{SER} - 4H_O^{SER} = 7GFFB - JFF$
${}^oG_{Fe^{2+}:Va:Va:O^{2-}} - H_{Fe}^{SER} - 4H_O^{SER} = 5GFFB + C$
${}^oG_{Fe^{3+}:Va:Va:O^{2-}} - H_{Fe}^{SER} - 4H_O^{SER} = 5GFFB - JFF + C$
${}^oG_{Mn^{2+}:Mn^{2+}:Va:O^{2-}} - 3H_{Mn}^{SER} - 4H_O^{SER} = GM2M2B$
${}^oG_{Mn^{2+}:Mn^{3+}:Va:O^{2-}} - 3H_{Mn}^{SER} - 4H_O^{SER} = 7GMMB$
${}^oG_{Mn^{2+}:Mn^{4+}:Va:O^{2-}} - 3H_{Mn}^{SER} - 4H_O^{SER} = 14GMMB + JMMB - GM2M2B$
${}^oG_{Mn^{2+}:Va:Va:O^{2-}} - H_{Mn}^{SER} - 4H_O^{SER} = 8GGMN2O3B - 56GMMB - 3JMMB + 3GM2M2B + 2\,RT(6\ln(6) - 3\ln(3) - 2\ln(2))$
${}^oG_{Fe^{2+}:Mn^{2+}:Va:O^{2-}} - 2H_{Mn}^{SER} - H_{Fe}^{SER} - 4H_O^{SER} = 7GFFB - 7GMFB + GM2M2B$
${}^oG_{Fe^{2+}:Mn^{3+}:Va:O^{2-}} - 2H_{Mn}^{SER} - H_{Fe}^{SER} - 4H_O^{SER} = 7GFMB$
${}^oG_{Fe^{2+}:Mn^{4+}:Va:O^{2-}} - 2H_{Mn}^{SER} - H_{Fe}^{SER} - 4H_O^{SER} = 28GFMB + 2JFMB - 14GMMB - 7GFFB + JFF$
${}^oG_{Fe^{3+}:Mn^{2+}:Va:O^{2-}} - 2H_{Mn}^{SER} - H_{Fe}^{SER} - 4H_O^{SER} = 7GFFB - JFF - 7GMFB + GM2M2B$
${}^oG_{Fe^{3+}:Mn^{3+}:Va:O^{2-}} - 2H_{Mn}^{SER} - H_{Fe}^{SER} - 4H_O^{SER} = 7GFFB - JFF + 7GMMB - 7GMFB$
${}^oG_{Fe^{3+}:Mn^{4+}:Va:O^{2-}} - 2H_{Mn}^{SER} - H_{Fe}^{SER} - 4H_O^{SER} = 7GFFB - JFF + 14GMMB + JMMB - 7GMFB - GM2M2B$
${}^oG_{Mn^{2+}:Fe^{2+}:Va:O^{2-}} - H_{Mn}^{SER} - 2H_{Fe}^{SER} - 4H_O^{SER} = 14GFMB - 14GMMB - JMMB + 2JFMB + GM2M2B$
${}^oG_{Mn^{2+}:Fe^{3+}:Va:O^{2-}} - H_{Mn}^{SER} - 2H_{Fe}^{SER} - 4H_O^{SER} = 7GMFB$
${}^oG_{*:*:Fe^{2+}:O^{2-}} = {}^oG_{*:*:Va:O^{2-}} + 2GFFB - JFF + D$
${}^oG_{*:*:Mn^{2+}:O^{2-}} = {}^oG_{*:*:Va:O^{2-}} + 8GGMN1O1B - 2GM2M2B + 4\,RT\ln(2)$
Magnetic properties (p = 0.28):
for compounds containing only Fe cations $T_C = 848$ and $\beta = 44.54$
for compounds containing only Mn cations $T_C = 43.15^*$ and $\beta = 0^*$
for compounds containing Fe + Mn cations $T_C = 577^*$ and $\beta = 6^*$
${}^0\beta_{Mn^{2+}:Fe^{3+},Mn^{3+}:Va:O^{2-}} = 450^*$

α-Spinel: $(\mathbf{Fe^{2+}}, \mathbf{Fe^{3+}}, \mathbf{Mn^{2+}}, \mathbf{Mn^{3+}})_1(\mathbf{Fe^{2+}}, \mathbf{Fe^{3+}}, \mathbf{Mn^{2+}}, \mathbf{Mn^{3+}}, \mathbf{Va})_2(\mathbf{Fe^{2+}}, \mathbf{Mn^{2+}}, \mathbf{Va})_2(\mathbf{O^{2-}})_4$

${}^oG_{Fe^{2+}:Fe^{2+}:Va:O^{2-}} - 3H_{Fe}^{SER} - 4H_O^{SER} = 7GFFA + JFF$
${}^oG_{Fe^{3+}:Fe^{2+}:Va:O^{2-}} - 3H_{Fe}^{SER} - 4H_O^{SER} = 7GFFA$
${}^oG_{Fe^{2+}:Fe^{3+}:Va:O^{2-}} - 3H_{Fe}^{SER} - 4H_O^{SER} = 7GFFA$
${}^oG_{Fe^{3+}:Fe^{3+}:Va:O^{2-}} - 3H_{Fe}^{SER} - 4H_O^{SER} = 7GFFA - JFF$
${}^oG_{Fe^{2+}:Va:Va:O^{2-}} - H_{Fe}^{SER} - 4H_O^{SER} = 5GFFA + C$
${}^oG_{Fe^{3+}:Va:Va:O^{2-}} - H_{Fe}^{SER} - 4H_O^{SER} = 5GFFA - JFF + C$
${}^oG_{Mn^{2+}:Mn^{2+}:Va:O^{2-}} - 3H_{Mn}^{SER} - 4H_O^{SER} = 21GMMA + 2JMMA - 2GM3M3A$
${}^oG_{Mn^{3+}:Mn^{2+}:Va:O^{2-}} - 3H_{Mn}^{SER} - 4H_O^{SER} = 14GMMA + 2JMMA - GM3M3A$
${}^oG_{Mn^{2+}:Mn^{3+}:Va:O^{2-}} - 3H_{Mn}^{SER} - 4H_O^{SER} = 7GMMA$
${}^oG_{Mn^{3+}:Mn^{3+}:Va:O^{2-}} - 3H_{Mn}^{SER} - 4H_O^{SER} = GM3M3A$
${}^oG_{Mn^{2+}:Va:Va:O^{2-}} - H_{Mn}^{SER} - 4H_O^{SER} = 8GGMN2O3A - 6GM3M3A + 7GMMA + 2RT(6\ln(6) - 5\ln(5))$
${}^oG_{Mn^{3+}:Va:Va:O^{2-}} - H_{Mn}^{SER} - 4H_O^{SER} = 8GGMN2O3A - 5GM3M3A + 2RT(6\ln(6) - 5\ln(5))$
${}^oG_{Fe^{2+}:Mn^{2+}:Va:O^{2-}} - 2H_{Mn}^{SER} - H_{Fe}^{SER} - 4H_O^{SER} = 7GFMA + 14GMMA + 2JMMA - 2GM3M3A + 4RT\ln(2)$
${}^oG_{Fe^{2+}:Mn^{3+}:Va:O^{2-}} - 2H_{Mn}^{SER} - H_{Fe}^{SER} - 4H_O^{SER} = 7GFMA$

Table 2 continued

$^{o}G_{Fe^{3+}:Mn^{2+}:Va:O^{2-}} - 2H^{SER}_{Mn} - H^{SER}_{Fe} - 4H^{SER}_{O} = 21GMMA + 2JMMA + 7GFFA - JFF - 7GMFA - 2GM3M3A + 4RT\ln(2)$
$^{o}G_{Fe^{3+}:Mn^{3+}:Va:O^{2-}} - 2H^{SER}_{Mn} - H^{SER}_{Fe} - 4H^{SER}_{O} = 7GFMA - JFF$
$^{o}G_{Mn^{2+}:Fe^{2+}:Va:O^{2-}} - H^{SER}_{Mn} - 2H^{SER}_{Fe} - 4H^{SER}_{O} = 7GFFA + JFF + 7GMMA - 7GFMA$
$^{o}G_{Mn^{2+}:Fe^{3+}:Va:O^{2-}} - H^{SER}_{Mn} - 2H^{SER}_{Fe} - 4H^{SER}_{O} = 7GMFA$
$^{o}G_{Mn^{3+}:Fe^{2+}:Va:O^{2-}} - H^{SER}_{Mn} - 2H^{SER}_{Fe} - 4H^{SER}_{O} = 7GFFA + JFF - 7GFMA + GM3M3A$
$^{o}G_{Mn^{3+}:Fe^{3+}:Va:O^{2-}} - H^{SER}_{Mn} - 2H^{SER}_{Fe} - 4H^{SER}_{O} = 7GFFA - 7GFMA + GM3M3A$
$^{o}G_{*:*:Fe^{2+}:O^{2-}} = {}^{o}G_{*:*:Va:O^{2-}} + 2GFFA - JFF + D$
$^{o}G_{*:*:Mn^{2+}:O^{2-}} = {}^{o}G_{*:*:Va:O^{2-}} + 8GGMN1O1A - 42GMMA - 4JMMA + 4GM3M3A + 4RT\ln(2)$
Magnetic properties ($p = 0.28$):
for compounds containing only Fe cations $T_C = 848$ and $\beta = 44.54$
for compounds containing only Mn cations $T_C = 43.15^*$ and $\beta = 0^*$
for compounds containing Fe + Mn cations $T_C = 577^*$ and $\beta = 6^*$
$^{0}\beta_{Mn^{2+}:Fe^{3+},Mn^{3+}:Va:O^{2-}} = 450^*$

Functions

GFELIQ ($298.15 < T < 1811$) = $12040.17 - 6.55843T - 3.6751551E{-}21T^7$ + GHSERFE
GFELIQ ($1811 < T < 6000$) = $-10838.83 + 291.302T - 46T\ln(T)$
GFEOLIQ = $-137252 + 224.641T - 37.1815T\ln(T)$
GMN_L ($298.15 < T < 1519$) = GHSERMN + $17859.91 - 12.6208T - 4.41929E{-}21T^7$
GMN_L ($1519 < T < 6000$) = GHSERMN + $18739.51 - 13.2288T - 1.656847E{+}30T^{-9}$
GMN1O1_L = GMN1O1 + $43947 - 20.628T$
GMN1O1 = $-402478 + 259.356T - 46.835T\ln(T) - .00385T^2 + 212922/T$
GMN2O3_L = +2GMN1O1 + 0.5GO2GAS − $64953 + 43.144T$
GHSERMN ($298.15 < T < 1519$) = $-8115.28 + 130.059T - 23.4582T\ln(T) - 0.00734768T^2 + 69827.1/T$
GHSERMN ($1519 < T < 6000$) = $-28733.41 + 312.2648T - 48T\ln(T) + 1.656847E{+}30/T^9$
GHSERFE ($298.15 < T < 1811$) = $1225.7 + 124.134T - 23.5143T\ln(T) - 0.00439752T^2 - 5.8927E{-}08T^3 + 77359/T$
GHSERFE ($1811 < T < 6000$) = $-25383.581 + 299.31255T - 46T\ln(T) + 2.29603E{+}31/T^9$
GO2GAS ($298.15 < T < 1000$) = $-6961.74451 - 51.0057202T - 22.2710136T\ln(T) - 0.0101977469T^2 + 1.32369208E{-}06T^3 - 76729.7484/T$
GO2GAS ($1000 < T < 3300$) = $-13137.5203 + 25.3200332T - 33.627603T\ln(T) - 0.00119159274T^2 + 1.35611111E{-}08T^3 + 525809.556/T$
GO2GAS ($3300 < T < 6000$) = $-27973.4908 + 62.5195726T - 37.9072074T\ln(T) - 8.50483772E{-}04T^2 + 2.14409777E{-}08T^3 + 8766421.4/T$
AWUSTITE = $-55384 + 27.888T$
GWUSTITE = $-279318 + 252.848T - 46.12826T\ln(T) - 0.0057402984T^2$
GFE2O3 = $-858683 + 827.946T - 137.0089T\ln(T) + 1453810/T$
GMN2O3 = $-998618 + 588.619T - 101.956T\ln(T) - .018844T^2 + 589055/T$
JFF = $46826 - 27.266T$
C = $120730 - 20.102T$
D = $402520 - 30.529T$
GFFB = $-161731 + 144.873T - 24.9879T\ln(T) - 0.0011952256T^2 + 206520/T$
GFMB = GMN2O3/7 + GWUSTITE/7*
GMFB = $-182450 + 133T - 23.099T\ln(T) - 0.0014T^2 + 124000/T$*
GMMB = GMN3O4B/7 + GMN3O4A/7*
GMN3O4A = $-1439700 + 892.2T - 154.748T\ln(T) - 0.017408T^2 + 986139/T$*
GMN3O4B = $15270 + 7T$*
JMMB = $26210 - 17.46T$*
JMFB = 28000*
JFMB = −27000*
GGMN1O1B = GMN1O1 + $41500 - 10.25T$*
GGMN2O3B = GMN2O3 + $192300 - 193.8T + 0.05T^2$*
GM2M2B = 21GMFB + 2JMFB − 14GFFB + 2JFF*
GFFA = GFFB + 1000
GFMA = GFMB*
GMFA = GMFB + $4900 - 1.9T$*
GMMA = GMN3O4A/7*
JMMA = 95000*
JMFA = 28000*

Table 2 continued

GGMN1O1A = GMN1O1 + 58500 – 11*T**
GGMN2O3A = GMN2O3 + 240000 – 211.8*T* + 0.05T^2*
GM3M3A = 10.5GMMA + JMMA – 10.5GMFA – JMFA + 7GFFA – JFF*

* indicates parameters assessed in this work
Parameters for the metallic phases and the gas phase can be found elsewhere[10,12,116]

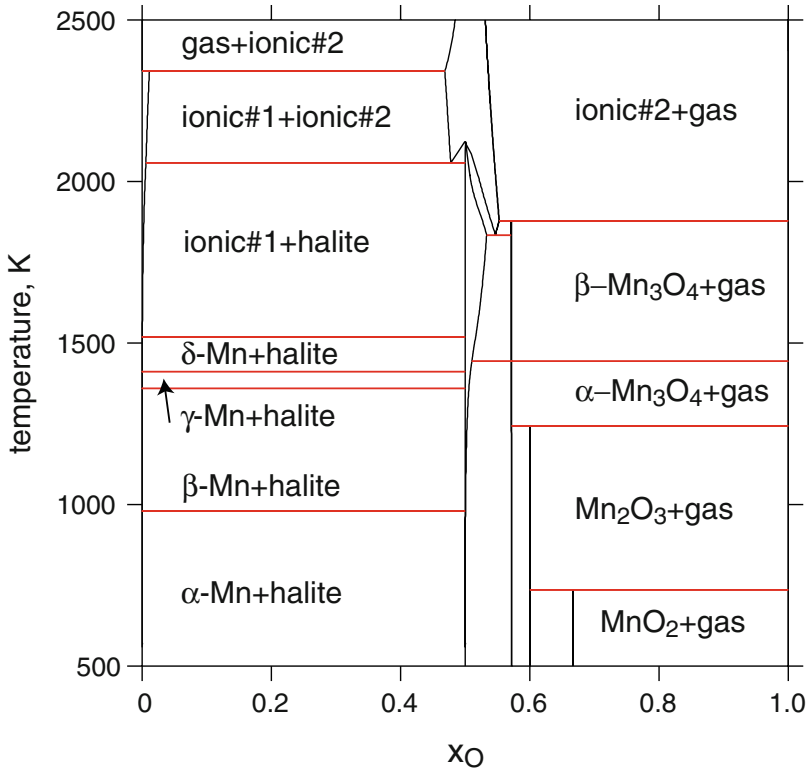

Fig. 1 Calculated Mn-O phase diagram at 1 atmosphere total pressure

neutron diffraction investigations at elevated temperatures between 603 and 1443 K. Hasting and Corliss[93] found the degree of inversion to be independent of preparation conditions and temperature. Other authors found a very low degree of inversion.[118,119] Faller and Birchenall[120] showed that in some cases even rapid quenching is not sufficient to retain the equilibrium distribution of cations corresponding to the annealing temperature. Therefore, the experimental data on the degree of inversion (fraction of Mn ions in octahedral sites) from Jirák and Vratislav was used to evaluate the cation distribution in $MnFe_2O_4$. $MnFe_2O_4$ is known to be an almost normal spinel at room temperature with Mn^{2+} ions on tetrahedral sites and Fe^{3+} ions on octahedral sites. At increasing temperature the degree of inversion increases. The distribution of cations is determined by the formula $Mn_{1-\lambda}Fe_\lambda[Mn_\lambda Fe_{2-\lambda}]O_4$, where the cations inside the square brackets are in octahedral sites while the cations in front of the brackets are in tetrahedral sites. The calculated degree of inversion is shown in Fig. 8. The calculated cation distribution in cubic $Fe_{3-x}Mn_xO_4$ at 1000 K is shown in Fig. 9, where the tetragonal spinel phase was excluded in the calculation. Terayama et al.[100] found a wide nonstoichiometric range in $MnFe_2O_4$ at 1153 K, corresponding to $-0.2258 \le \delta \le 0$ in $(Fe_xMn_{1-x})_{3-\delta}O_4$. This huge deviation from stoichiometry seems very unlikely and disagrees with the measurements from Bulgakova and Rozanov,[74] whose results agree well with our calculated values, even though they were not taken into account in this optimization, see Fig. 10.

The nonstoichiometry of $(Fe_{1-x}Mn_x)_{1-\delta}O$ at 1273 and 1473 K for different values on x, investigated by Subramanian and Dieckmann[72] and Franke and Dieckmann,[69] were used to optimize the interaction parameters in halite.

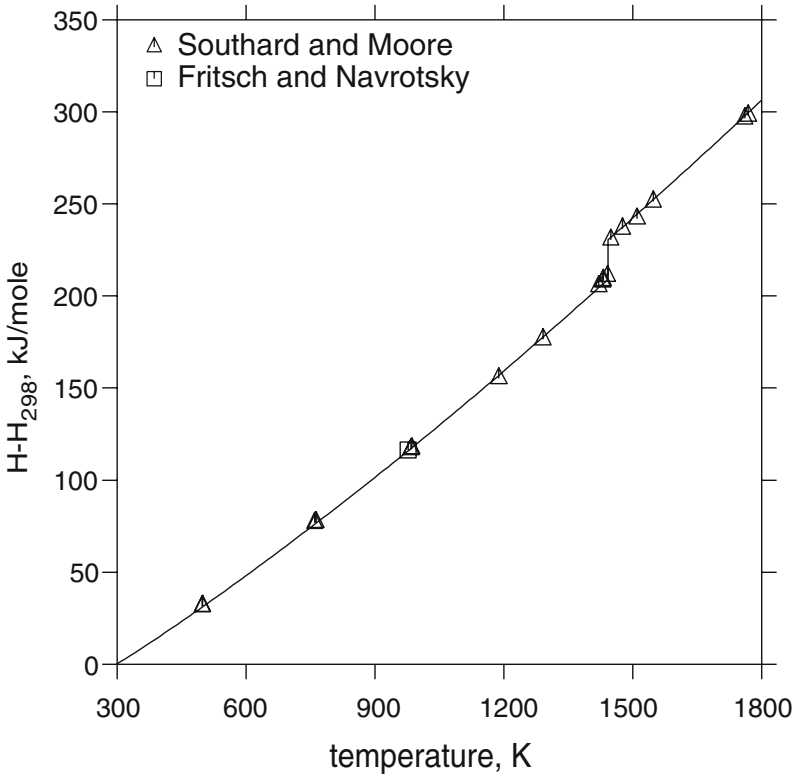

Fig. 2 Calculated and experimental[28,66] enthalpy of Mn_3O_4

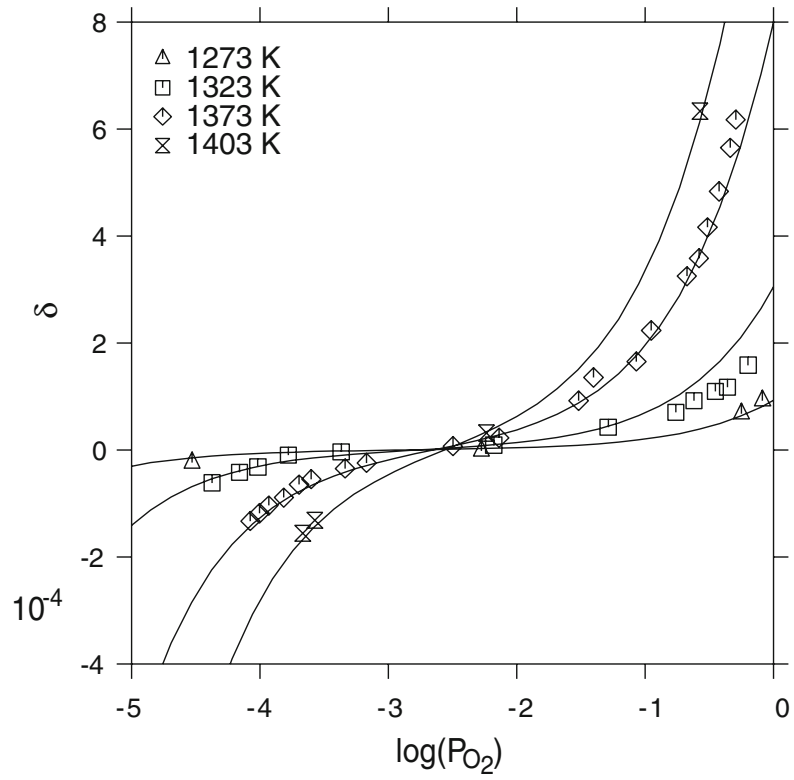

Fig. 3 Calculated and experimental[30] oxygen potential in α-$Mn_{3-\delta}O_4$

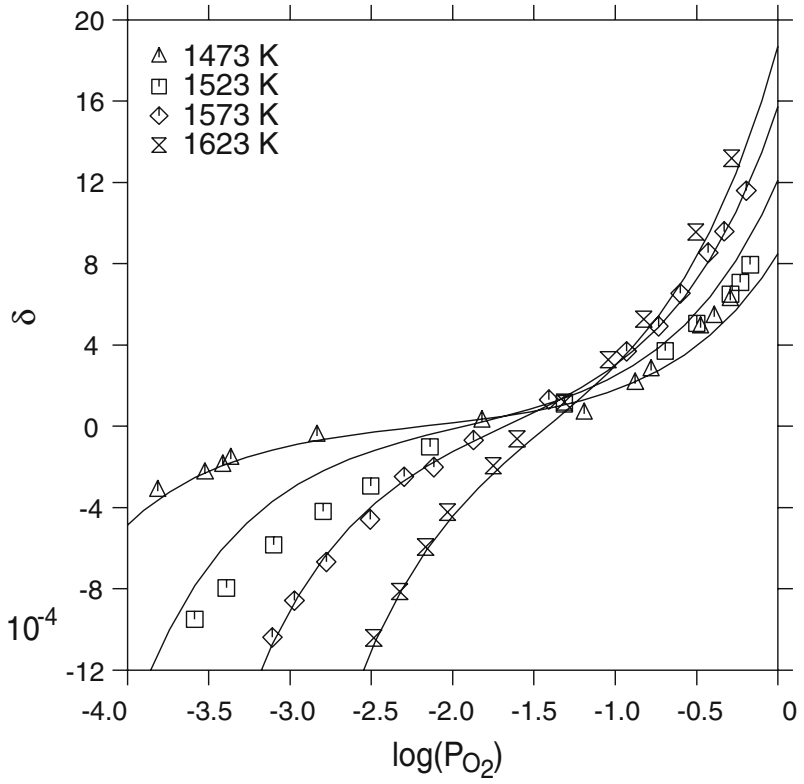

Fig. 4 Calculated and experimental[30] oxygen potential in β-$Mn_{3-\delta}O_4$

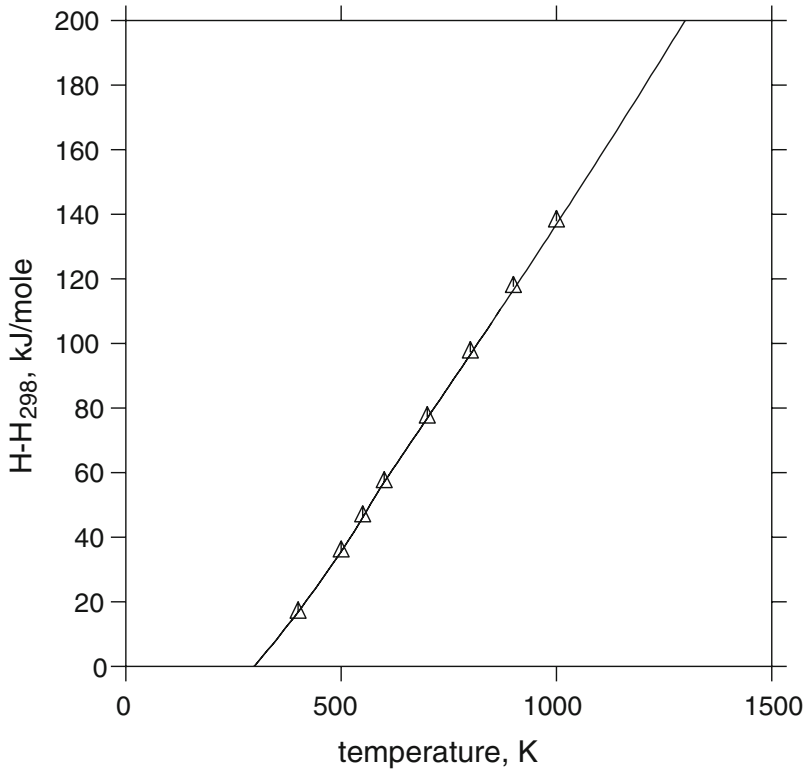

Fig. 5 Calculated and experimental[101] enthalpy of $MnFe_2O_4$

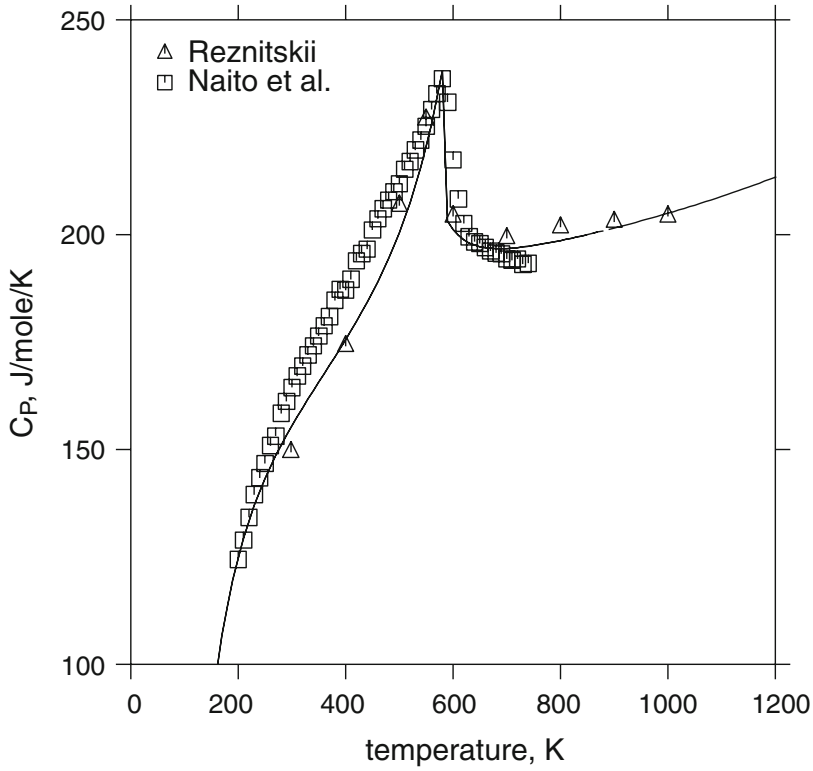

Fig. 6 Calculated and experimental[101,102] heat capacity of $MnFe_2O_4$

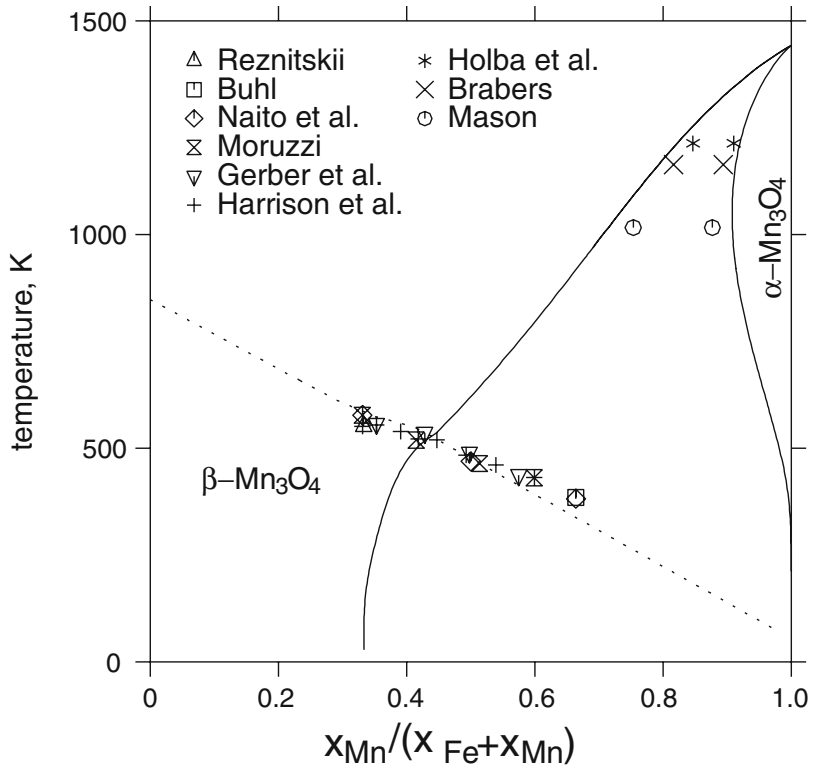

Fig. 7 Calculated and experimental[89-91,101-106] phase diagram and Curie temperature between Fe_3O_4 and Mn_3O_4

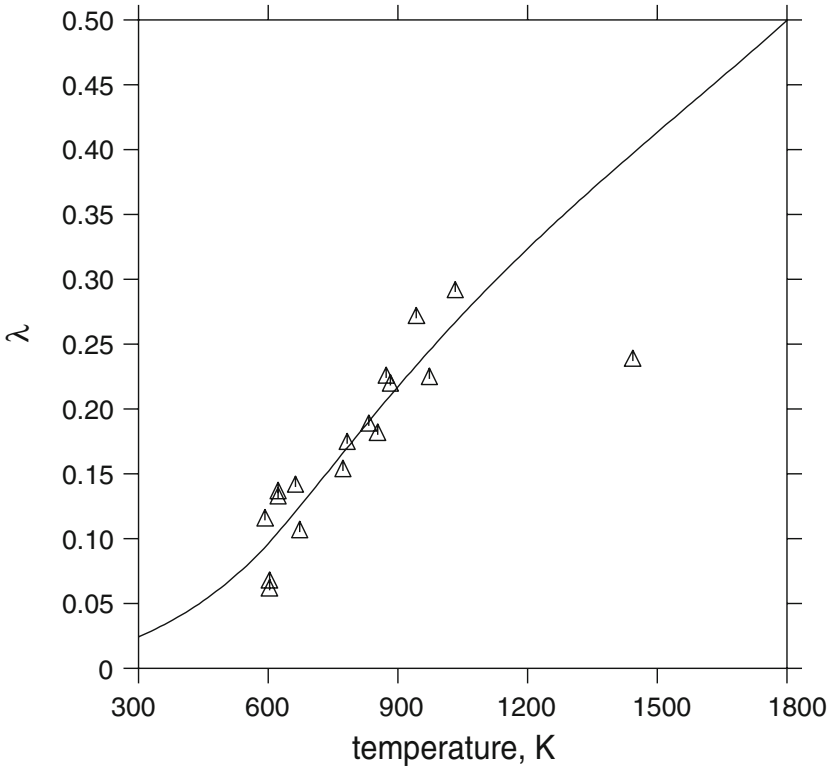

Fig. 8 Calculated and experimental[97] degree of inversion of $MnFe_2O_4$ ($Mn_{1-\lambda}Fe_{\lambda}[Mn_{\lambda}Fe_{2-\lambda}]O_4$)

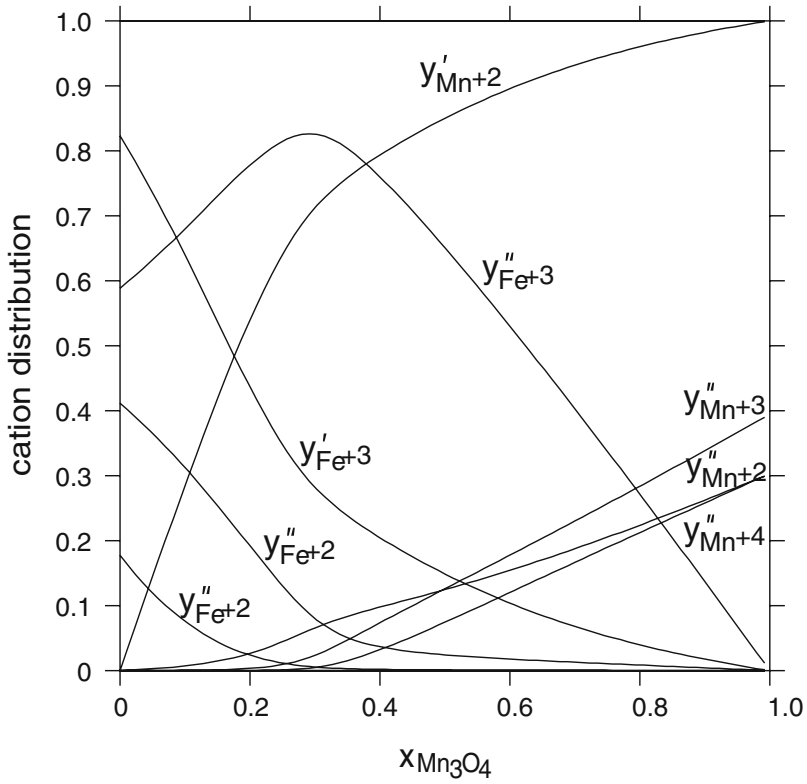

Fig. 9 Calculated cation distribution in cubic Fe_3O_4-Mn_3O_4 at 1000 K

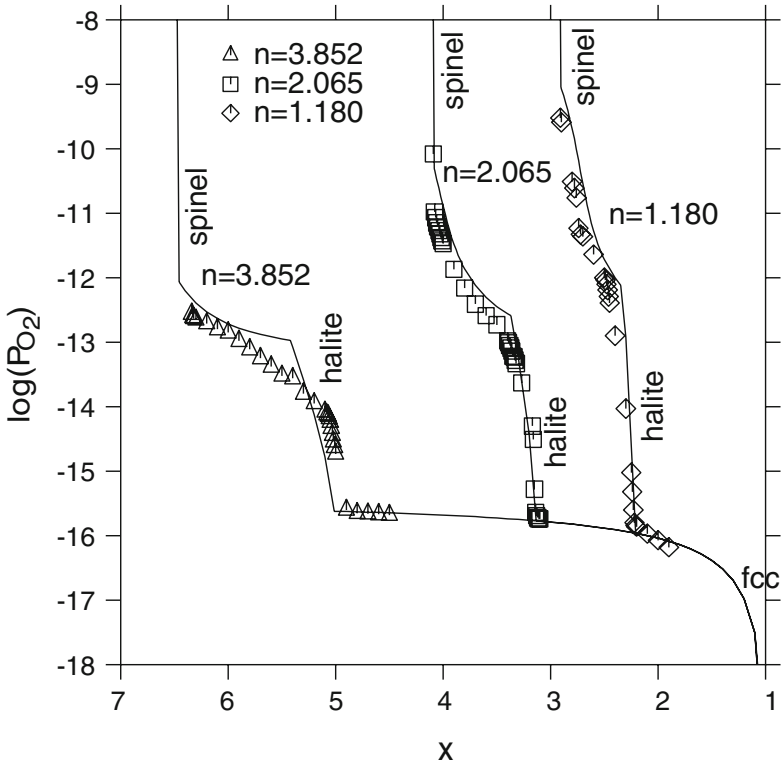

Fig. 10 Calculated and experimental[74] oxygen potential at 1242 K in $MnFe_nO_x$

The calculated partial pressure of oxygen in nonstoichiometric halite is shown in Fig. 11 and 12. It could be noted that the slope of the calculations does not perfectly align with the experiments. To change the slope of the calculated curves, the model for the manganowustite phase needs to be changed to also include Mn^{4+} ions.

When reasonable parameters had been given to the halite and spinel phases, experimental information on invariant equilibria was included in the assessment. Information from Subramanian and Dieckmann,[72] Franke and Dieckmann[69] and Schwerdtfeger and Muan[52] of the two-phase regions of halite/fcc and halite/spinel at two temperatures (1273 and 1473 K) were used to further improve the description of halite and spinel. Figure 13 shows the calculated composition-oxygen activity phase diagram at 1273 K together with experimental data.

The investigations of the two-phase regions of corundum/bixbyite and corundum/spinel from Ref 69, 75, 84, 86, 121 were used to describe the solubility of Mn in Fe_2O_3. The data from Bergstein and Kleinert[85] on the β-spinel/corundum phase boundary at 1273 K could not be reproduced. To correctly describe the solubility of Fe in Mn_2O_3, an excess parameter was required to be able to reproduce the experimental data. A phase diagram calculated in air (P = 0.21 bar) is shown in Fig. 14 together with experimental data.

The liquid phase is optimized using the data from Muan and Somiya[84] and Nölle[107] on the phase boundaries between liquid oxide and spinel/halite respectively. The experiments on the solubility of oxygen in the metallic melt are not taken into consideration in this assessment due to the large scattering. The experimental and calculated oxygen content of the metallic liquid in equilibrium with the halite phase are shown in Fig. 15.

Calculated isothermal sections at two different temperatures are shown in Fig. 16 and 17.

9. Conclusions and Discussion

The present assessment gives a good description of the available experimental information in the ternary Fe-Mn-O system. A complete list of all parameters is found in Table 2. Part of the Mn-O system has been revised. In the liquid phase the Mn^{3+} ion has been replaced by a neutral $MnO_{1.5}$ species equivalent to the Fe-O system. The spinel phases (α- and β-Mn_3O_4) are here modelled using a more complex description than the previous assessment from Grundy et al.[11] The new model describes the cation distribution of ions between tetrahedral and octahedral sites and the nonstoichiometry of the phases. The description of the spinel phases in the Fe-Mn-O system is consistent with the description of the Fe-Cr-Ni-O spinel from an earlier work,[1] but to be able to do thermodynamic calculations in the Fe-Cr-Mn-Ni-O system the Cr-Mn-O and Mn-Ni-O

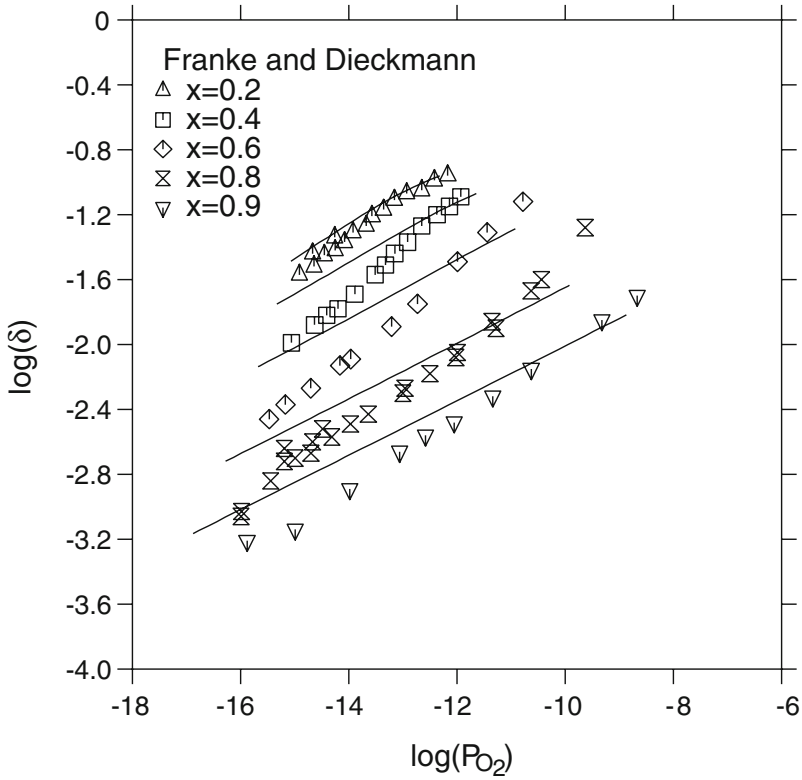

Fig. 11 Calculated and experimental[69] oxygen potential in $(Fe_{1-x}Mn_x)_{1-\delta}O$ at 1273 K

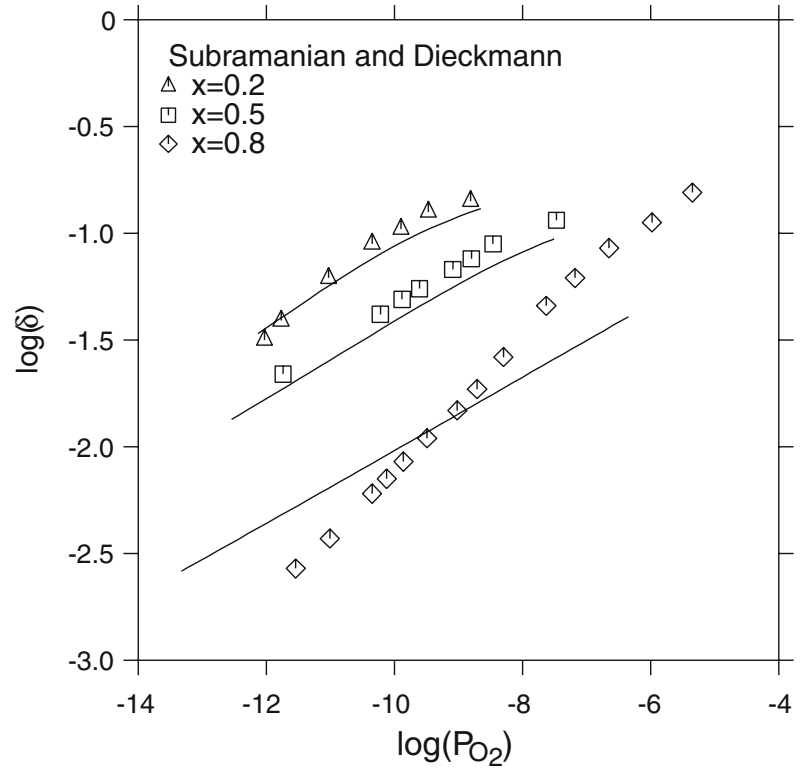

Fig. 12 Calculated and experimental[72] oxygen potential in $(Fe_{1-x}Mn_x)_{1-\delta}O$ at 1473 K

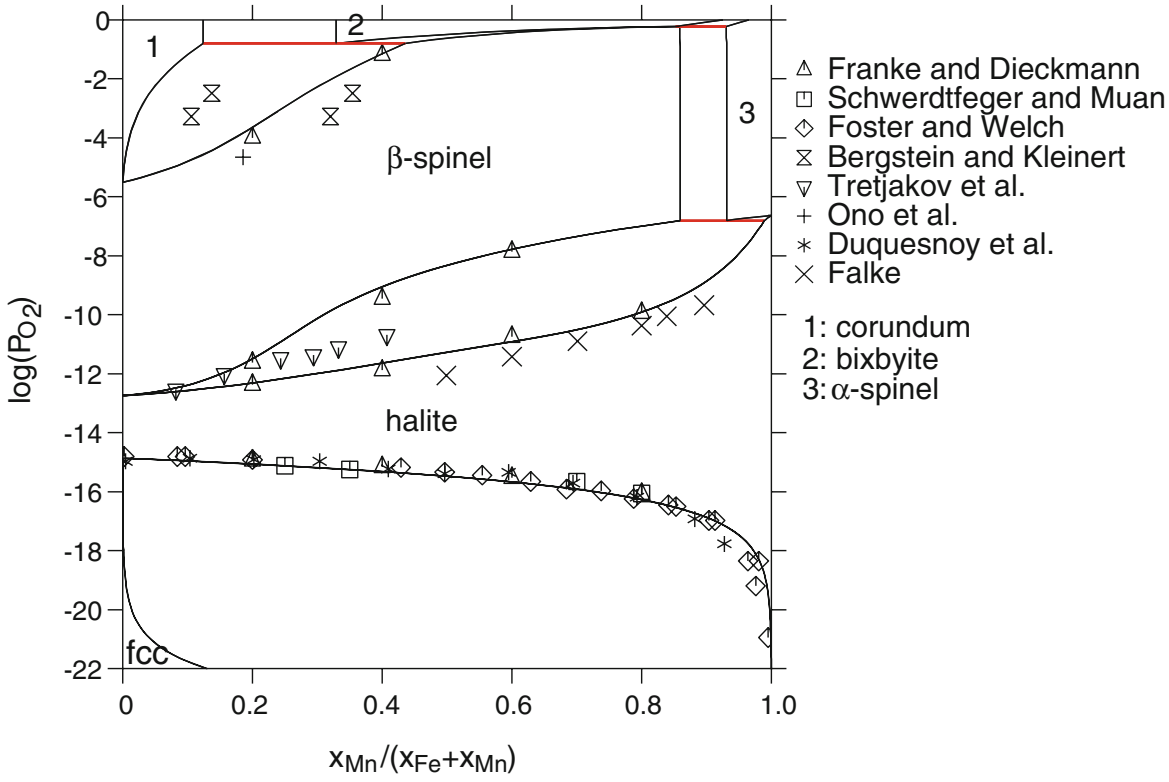

Fig. 13 Calculated and experimental[52,69,73,75-77,85,121] phase diagram at 1273 K

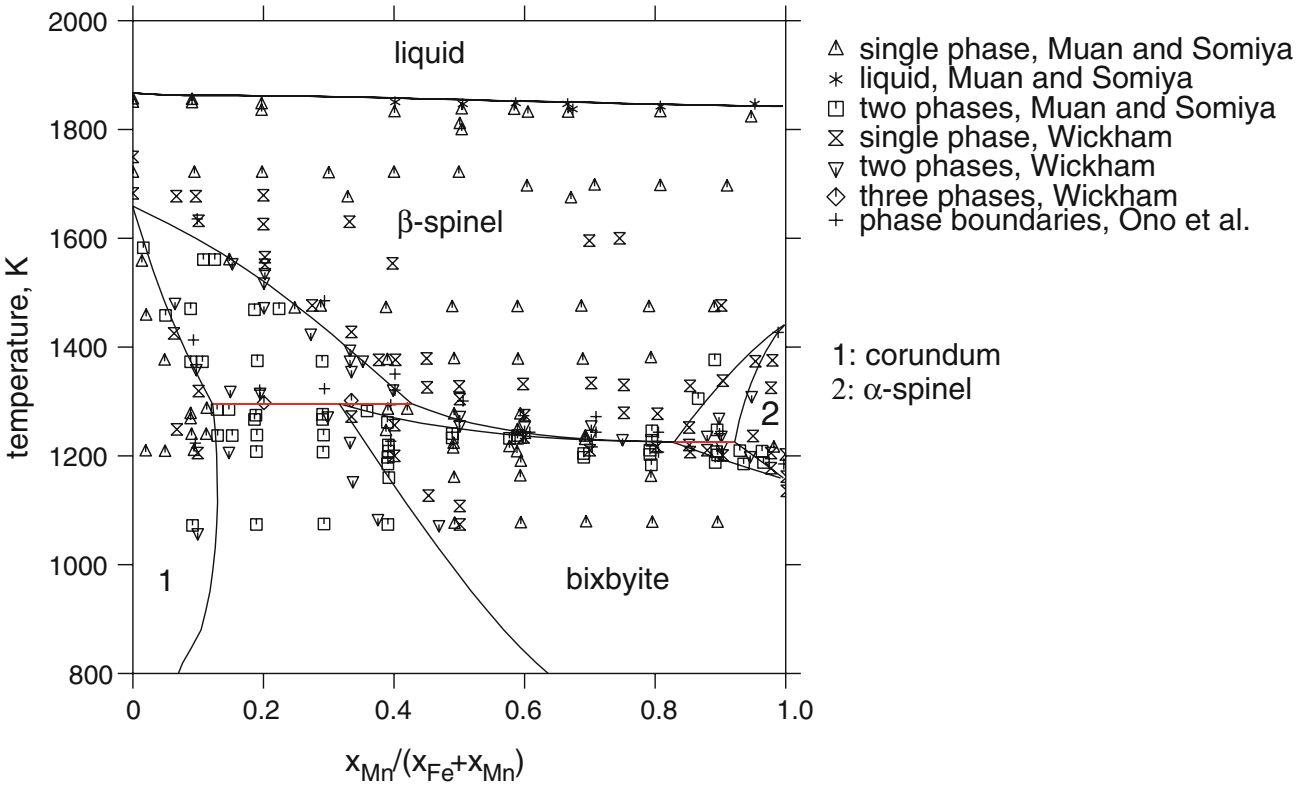

Fig. 14 Calculated and experimental[75,84,86] phase diagram for a fixed oxygen partial pressure of 0.21 bar

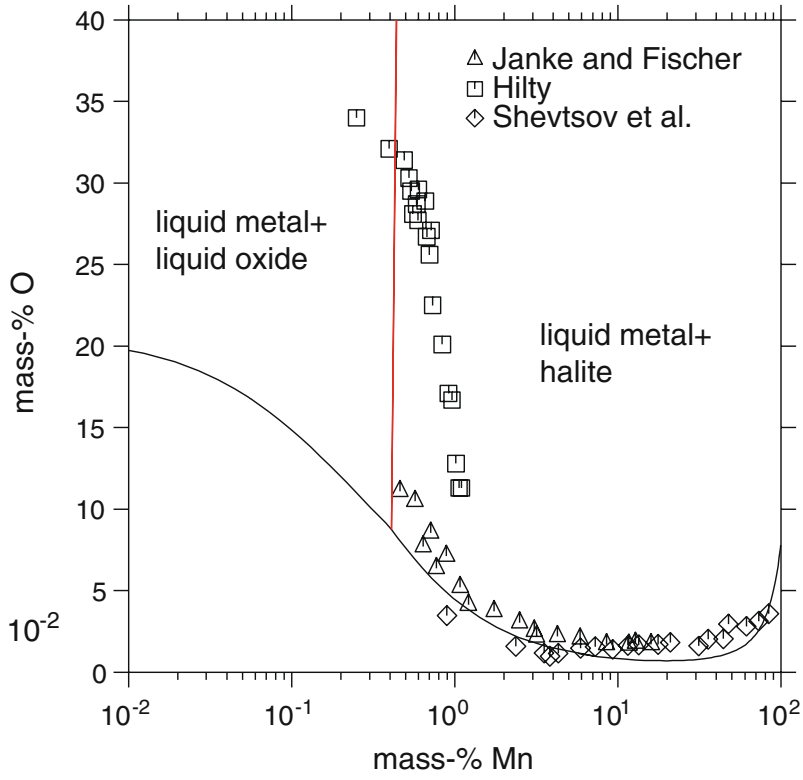

Fig. 15 Calculated and experimental[108,109,112] oxygen solubility in liquid Fe-Mn in equilibrium with halite and liquid oxide at 1873 K

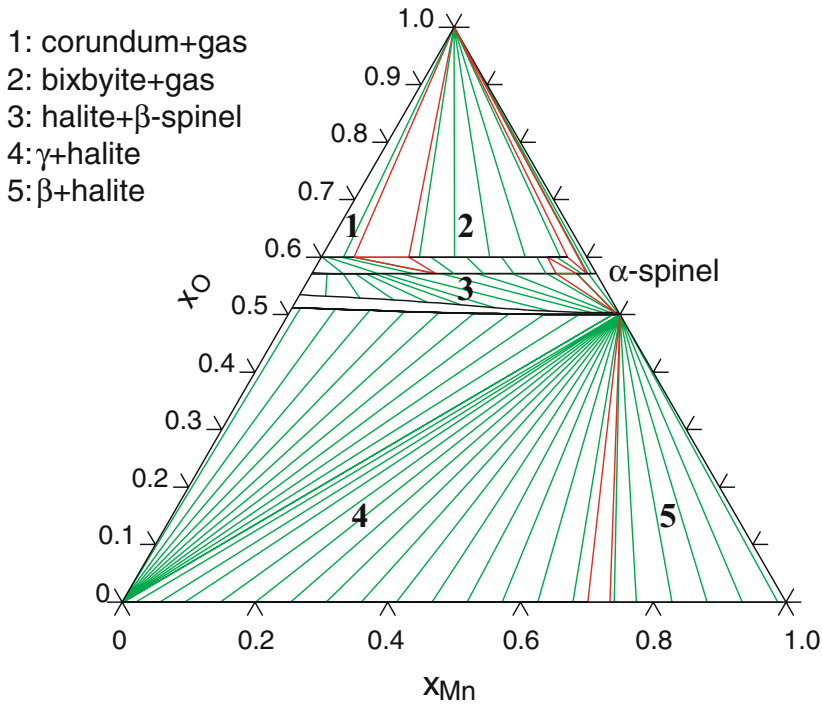

Fig. 16 Calculated isothermal section of the Fe-Mn-O system at 1273 K

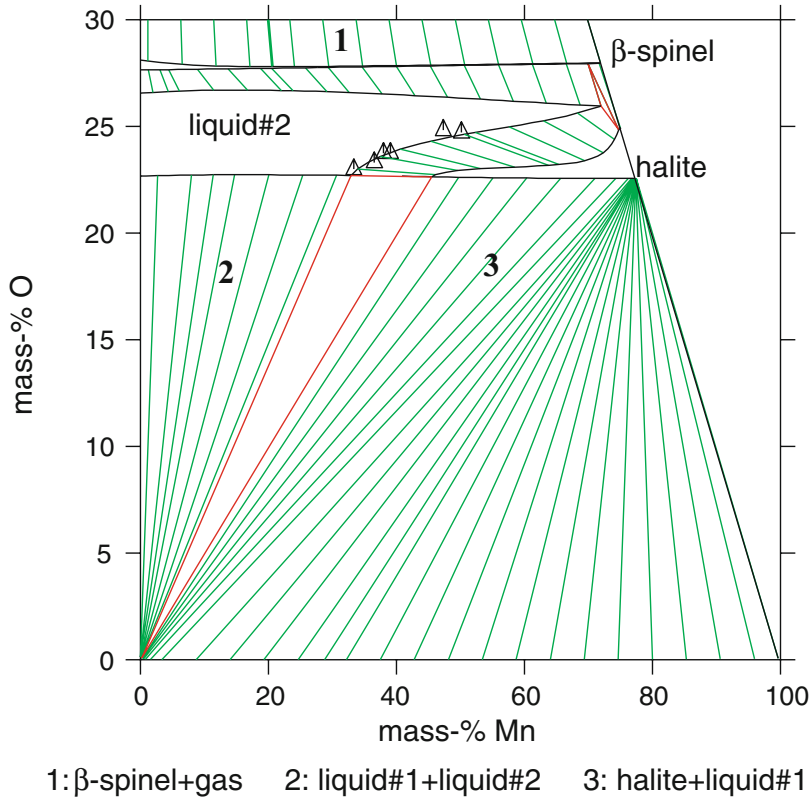

Fig. 17 Calculated isothermal section of the Fe-Mn-O system at 1823 K with experimental data from Nölle[107]

systems need to be assessed. The models in this work are compatible with the models used in a parallel work on the Al_2O_3-CaO-Fe-O-MgO-SiO_2 system.[122,123]

Acknowledgments

Bengt Hallstedt is acknowledged for providing files and information regarding the Mn-O system. The authors are grateful to Dr Huahai Mao for valuable discussions. This work was financially supported by the Swedish Steel Producers Association.

References

1. L. Kjellqvist, M. Selleby, and B. Sundman, Thermodynamic Modelling of the Cr-Fe-Ni-O System, *CALPHAD*, 2008, **32**, p 577-592
2. L. Kjellqvist and M. Selleby, Adding C to the Thermodynamic Description of the Cr-Fe-Ni-O System, *CALPHAD*, 2009, **33**, p 393-397
3. M. Hillert, B. Jansson, B. Sundman, and J. Ågren, A Two-Sublattice Model for Molten Solutions with Different Tendency for Ionization, *Metall. Trans. A*, 1985, **16A**, p 261-266
4. B. Sundman, Modification of the Two-Sublattice Model for Liquids, *CALPHAD*, 1991, **15**, p 109-119
5. M. Hillert, The Compound Energy Formalism, *J. Alloys Compd.*, 2001, **320**, p 161-176
6. N. Saunders and A.P. Miodownik, *CALPHAD (Calculation of Phase Diagrams): A Comprehensive Guide*, 1998
7. H. Lukas, S.G. Fries, and B. Sundman, *Computational Thermodynamics, The CALPHAD Method*, 2007
8. B. Sundman, An Assessment of the Fe-O System, *J. Phase Equilib.*, 1991, **12**, p 127-140
9. M. Selleby and B. Sundman, A Reassessment of the Ca-Fe-O System, *CALPHAD*, 1996, **20**, p 381-392
10. M. Kowalski and P.J. Spencer, Thermodynamic Reevaluation of the Cr-O, Fe-O and Ni-O Systems: Remodelling of the Liquid, bcc and fcc Phases, *CALPHAD*, 1995, **19**, p 229-243
11. A.N. Grundy, B. Hallstedt, and L.J. Gauckler, Assessment of the Mn-O System, *J. Phase Equilib.*, 2003, **24**, p 21-39
12. W. Huang, An Assessment of the Fe-Mn System, *CALPHAD*, 1989, **13**, p 243-252
13. R. Weiland, "Untersuchungen zur thermodynamik oxidescher lösungsphasen im system Co-Fe-Mn-O," Doctoral Thesis, Stuttgart, 2002
14. A.D. Pelton, H. Schmalzried, and J. Sticher, Thermodynamics of Mn_3O_4-Co_3O_4, Fe_3O_4-Mn_3O_4, and Fe_3O_4-Co_3O_4 Spinels by Phase Diagram Analysis, *Ber. Bunsenges. Phys. Chem.*, 1979, **83**, p 241-252
15. G. Inden, Determination of Chemical and Magnetic Interchange Energies in BCC Alloys. I. General Treatment, *Z. Metallkd.*, 1975, **66**, p 577-582
16. M. Hillert and M. Jarl, A Model for Alloying Effects in Ferromagnetic Metals, *CALPHAD*, 1978, **2**, p 227-238
17. H. Mao, M. Selleby, and B. Sundman, A Re-evaluation of the Liquid Phases in the CaO-Al_2O_3 and MgO-Al_2O_3 Systems, *CALPHAD*, 2004, **28**, p 307-312

18. H.A. Jahn and E. Teller, Stability of Polyatomic Molecules in Degenerate Electronic States. I. Orbital Degeneracy, *Proc. R. Soc. Lond. A*, 1937, **161**, p 220-235
19. S.E. Dorris and T.O. Mason, Electrical Properties and Cation Valencies in Mn_3O_4, *J. Am. Ceram. Soc.*, 1988, **71**, p 379-385
20. F.C.M. Driessens, Place and Valence of the Cations in Mn_3O_4 and Some Related Manganates, *Inorg. Chim. Acta*, 1967, **1**, p 193-207
21. D.S. McClure, The Distribution of Transition Metal Cations in Spinels, *J. Phys. Chem. Solids*, 1957, **3**, p 311-317
22. J.D. Dunitz and L.E. Orgel, Electronic Properties of Transition-Metal Oxides—II. Cation Distribution Amongst Octahedral and Tetrahedral Sites, *J. Phys. Chem. Solids*, 1957, **3**, p 318-323
23. K.S. Irani, A.P.B. Sinha, and A.B. Biswas, Crystal Distortion in Spinels Containing Mn^{3+} Ions, *J. Phys. Chem. Solids*, 1960, **17**, p 101-111
24. M. Hillert, L. Kjellqvist, H. Mao, M. Selleby, and B. Sundman, Parameters in the Compound Energy Formalism for Ionic Systems, *CALPHAD*, 2009, **33**, p 227-232
25. L.B. Pankratz, Thermodynamic Properties of Elements and Oxides, Technical Report, Bureau of Mines Bulletin 672, 1982
26. A.V. Ramano Rao and V.B. Tare, Determination of Free Energy of Formation, Heat and Temperature of Transformation of Mn_3O_4, *Trans. Inst. Min. Metall. C*, 1973, **82**, p 34-37
27. K.S. Irani, A.P.B. Sinha, and A.B. Biswas, Effect of Temperature on the Structure of Manganites, *J. Phys. Chem. Solids*, 1962, **23**, p 711-727
28. J. Southard and G.E. Moore, High-Temperature Heat Content of Mn_3O_4, $MnSiO_3$ and Mn_3C, *J. Am. Chem. Soc.*, 1942, **64**, p 1769-1770
29. R. Metselaar, R.E.J. Van Tol, and P. Piercy, The Electrical Conductivity and Thermoelectric Power of Mn_3O_4 at High Temperatures, *J. Solid State Chem.*, 1981, **38**, p 335-341
30. M. Keller and R. Dieckmann, Defect Structure and Transport Properties of Manganese Oxides: (II) The Nonstoichiometry of Hausmannite ($Mn_{3-\delta}O_4$), *Ber. Bunsenges. Phys. Chem.*, 1985, **89**, p 1095-1104
31. A. Schmier and G. Sterr, Contribution to the Knowledge of the Hausmannite Phase, *Z. Anorg. Allg. Chem.*, 1966, **346**, p 181-187
32. H.J. Van Hook and M.L. Keith, The System Mn_3O_4-Fe_3O_4, *Am. Mineral.*, 1958, **43**, p 69-83
33. G. Trömel, W. Fix, K. Koch, and F. Schaberg, The Phase Diagram of the Manganese-Oxygen System, *Erzmetall.*, 1976, **29**, p 234-237
34. H.F. McMurdie and E. Golovato, Study of the Modifications of Manganese Dioxide, *J. Res. Nat. Bur. Stand.*, 1948, **41**, p 589-600
35. A.Z. Hed and D. Tannhauser, Contribution to the Mn-O Phase Diagram at High Temperature, *J. Electrochem. Soc.*, 1967, **114**, p 314-318
36. W.C. Hahn and A. Muan, Studies in the System Mn-O: The Mn_2O_3-Mn_3O_4-MnO Equilibria, *Am. J. Sci.*, 1960, **258**, p 66-78
37. R.W. Millar, The Specific Heats at Low Temperatures of Manganous Oxide, Manganous-Manganic Oxide and Manganese Dioxide, *J. Am. Chem. Soc.*, 1928, **50**, p 1875-1883
38. C.H. Shomate, Heats of Formation of Manganomanganic Oxide and Manganese Dioxide, *J. Am. Chem. Soc.*, 1943, **65**, p 785-789
39. N.G. Schmahl and F. Shenouda, The Thermal Decomposition of Manganese(III)-Oxide (Mn_2O_3), *Arch. Eisenhuttenw.*, 1963, **34**, p 511-518
40. C. Benedicks and J. Löfquist, *Non-Metallic Inclusions in Iron and Steel*, Chapman & Hall, London, 1930
41. M. Le Blanc and G.Z. Wehner, Contribution to the Knowledge of the Manganese Oxides, *Phys. Chem. Abt. A*, 1934, **168**, p 59-78
42. N.G. Schmahl and D.F.K. Hennings, The Phase Diagram of the Mn_3O_4-MnO System and its Pressures of Dissociation, *Arch. Eisenhuttenw.*, 1969, **40**, p 395-399
43. T.E. Moore, M. Ellis, and P.W. Selwood, Solid Oxides and Hydroxides of Manganese, *J. Am. Chem. Soc.*, 1959, **72**, p 856-866
44. N.G. Schmahl and D.F.K. Hennings, The Nonstoichiometry of the Manganese(II)-Oxide in Thermal Equilibrium, *Z. Phys. Chem.*, 1969, **63**, p 111-124
45. A. Bergstein and J. Vintera, The Thermal Decomposition of Manganese Carbonates, *Coll. Czech. Chem. Commun.*, 1956, **22**, p 884-895
46. D.R. Petzold, Züchtung und Eigenschaften von Mangan-, Kobalt-und Zinkmanganatkristallen, *Kristall und Technik*, 1971, **6**, p 53-57
47. H. Von Wartenberg, H.J. Reusch, and E. Saran, Schmelzpunktsdiagramme höchstfeuerfester Oxyde. VII. Systeme mit CaO und BeO, *Z. Anorg. Chem.*, 1937, **230**, p 257-276
48. C. Klingsberg and R. Roy, Solid-Solid and Solid-Vapor Reactions and a New Phase in the System Mn-O, *J. Am. Ceram. Soc.*, 1960, **43**, p 620-626
49. R.J. Meyer and K. Rötgers, Die Dissoziationstemperaturen der Manganoxyde MnO_2 und Mn_2O_3 in Luft und Sauerstoff, *Z. Anorg. Chem.*, 1908, **57**, p 104-112
50. H.E. Kissinger, H.F. McMurdie, and B.S. Simpson, Thermal Decomposition of Manganous and Ferrous Carbonates, *J. Am. Ceram. Soc.*, 1956, **39**, p 168-172
51. T.R. Ingraham, Thermodynamics of the Mn-S-O System Between 1000°K and 1250°K, *Can. Metall. Quart.*, 1966, **5**, p 109-122
52. K. Schwerdtfeger and A. Muan, Equilibria in the System Fe-Mn-O Involving (Fe, Mn)O and $(Fe, Mn)_3O_4$ Solid Solutions, *Trans. Met. Soc. AIME*, 1967, **239**, p 1114-1119
53. H. Le Chatelier, Heat of Formation of Manganese Compounds, *C. R. Hebd. Seances Acad. Sci.*, 1896, **122**, p 80-82
54. O. Ruff and E. Gersten, Über die Carbide des Mangans und Nickels, *Ber. Deutsche Chem. Ges.*, 1913, **46**, p 400
55. W.A. Roth, Zur Thermochemie des Eisens, Mangans und Nickels, *Z. Angew. Chem.*, 1929, **42**, p 981-984
56. H. Siemonsen, Neubestimmung der bildungswaermen der manganoxyde, *Z. Elektrochem.*, 1939, **45**, p 637-645
57. H. Ulich and H. Siemonsen, Contribution to the Metallurgy of Manganese by Thermochemical Measurements and Equilibria Calculations, *Arch. Eisenhuttenw.*, 1940, **14**, p 27-34
58. A.D. Mah, Thermodynamic Properties of Manganese and its Compounds, Technical Report, Bureau of Mines Report of Investigations 5600, 1960
59. T.A. Zordan and L.G. Hepler, Thermochemistry and Oxidation Potentials of Manganese and its Compounds, *Chem. Rev.*, 1968, **68**, p 737-745
60. R.A. Robie and D.R. Waldbaum, Thermochemical Properties of Minerals and Related Substances at 298.15 K (25°C and One Atmosphere (1.013 Bars) Pressure and at Higher Temperatures, Technical Report, Geological Survey Bulletin 1259, 1968
61. O. Knacke, O. Kubaschewski, and K. Hesselmann, *Thermodynamic Properties of Inorganic Substances*, Springer-Verlag, Berlin, 1991

62. O. Kubaschewski, C.B. Alcock, and P.J. Spencer, *Materials Thermochemistry*, 6th ed., Pergamon Press, New York, 1993
63. H.S. O'Neill and M.I. Pownceby, Thermodynamic Data from the Redox Reactions at High Temperatures. I. An Experimental and Theoretical Assessment of the Electrochemical Method Using Stabilized Zirconia Electrolytes, with Revised Values for the Fe-'FeO', Co-CoO, Ni-NiO and Cu-Cu_2O Oxygen Buffers and New Data for the W-W02 Buffer, *Contrib. Mineral. Petrol.*, 1993, **114**, p 296-314
64. R.A. Robie and B.S. Hemingway, Low-Temperature Molar Heat Capacities and Entropies of MnO_2 (Pyrolusite), Mn_3O_4 (Hausmanite), and Mn_2O_3 (Bixbyite), *J. Chem. Thermodyn.*, 1985, **17**, p 165-187
65. K. Chhor, J.F. Bocquet, and C. Pommier, Heat Capacity and Thermodynamic Behaviour of Mn_3O_4 and $ZnMn_2O_4$ at Low Temperatures, *J. Chem. Thermodyn.*, 1986, **18**, p 89-99
66. S. Fritsch and A. Navrotsky, Thermodynamic Properties of Manganese Oxides, *J. Am. Ceram. Soc.*, 1996, **79**, p 1761-1768
67. H. O'Neill and A. Navrotsky, Cation Distribution and Thermodynamic Properties of Binary Spinel Solid Solutions, *Am. Mineral.*, 1984, **69**, p 733-753
68. H. Okinaka, K. Kosuge, and S. Kachi, Phase Diagram of (Fe,Mn)O at 1260 K, *J. Jpn. Soc. Powder Metall.*, 1968, **15**, p 295-301
69. P. Franke and R. Dieckmann, Thermodynamics of Iron Manganese Mixed Oxides at High Temperatures, *J. Phys. Chem. Solids*, 1990, **51**, p 49-57
70. A.A. Lykasov and M.S. Pavlovskaya, Thermodynamic Properties of Manganowustite, *Russ. J. Phys. Chem.*, 1988, **62**(5), p 602-605
71. H. Soliman and A. Stoklosa, Deviation from Stoichiometry of Mn-Doped Ferrous Oxide, *Solid State Ionics*, 1990, **42**, p 85-91
72. R. Subramanian and R. Dieckmann, Nonstoichiometry and Thermodynamics of the Solid Solution (Fe, Mn)1-deltaO at 1200°C, *J. Phys. Chem. Solids*, 1993, **54**, p 991-1000
73. P.K. Foster and A.J.E. Welch, Metal-Oxide Solid Solutions: Part 2. Activity Relationships in Solid Solutions of Ferrous Oxide and Manganous Oxide, *Trans. Faraday Soc.*, 1956, **52**, p 1636-1642
74. T.I. Bulgakova and A.G. Rozanov, Phase Equilibria in the Ferrite Region of the Mn-Fe-O System, *Russ. J. Phys. Chem.*, 1970, **44**, p 385-388
75. K. Ono, T. Ueda, Y. Ozaki, A. Yamaguchi, and J. Moriyama, Thermodynamic Study of the Iron-Manganese-Oxygen System, *J. Jpn. Inst. Met.*, 1971, **35**, p 757-763
76. A. Duquesnoy, J. Couzin, and P. Gode, Isothermal Representation of Ternary Phase Diagrams A-B-O. Study of the System Mn-Fe-O, *C. R. Acad. Sci. Paris C*, 1975, **281**, p 107-109
77. H. Falke, "Innere Reduktion von (Fe,Mn)1O Mischoxiden," Doctoral Thesis, Universität Hannover, 1987
78. I.V. Gordeev, Y.D. Tret'yakov, and K.G. Khomyakov, Thermodynamic Properties of Solid Solutions in the System Fe_3O_4-Mn_3O_4, *Zh. Neorg. Khim.*, 1964, **9**, p 164-168
79. K.H. Ulrich, K. Bohnenkamp, and H.J. Engell, Über die Gleichgewichte von Magnetit-Hausmannit-Mischkristallen mit Wüstit-Mangan(II)oxid-Mischkristallen und Sauerstoff und die Reduktion von Magnetit-Hausmannit-Mischoxiden, *Z. Phys. Chem.*, 1966, **51**, p 35-49
80. B. Punge-Witteler, Phasengleichheit zwischen Spinell und Wüstit im System Fe-Mn-O bei 700°C, 1 bar, *Z. Phys. Chem.*, 1984, **142**, p 239-248
81. S. Takeuchi, K. Furukawa, and K. Gunji, Statistico-Thermodynamical Studies on Oxidation and Reduction Equilibriums of Mn-Wüstite with Gas Phases, *J. Jpn. Inst. Met.*, 1960, **24**, p 187
82. H.J. Engell, Equilibrium Measurements on Oxide Mixed Crystals, *Z. Phys. Chem.*, 1962, **35**, p 192-195
83. W. Ringsdorf, "Gleichgewichtsverschiebungen im System Eisen-Sauerstoff durch Legierungs- und Mischkristallbildung mit Nickel, Mangan und Kobalt bzw. deren Oxiden," Doctoral Thesis, Universität des Saarlandes, Saarbrucken, 1964
84. A. Muan and S. Somiya, The System Iron Oxide-Manganese Oxide in Air, *Am. J. Sci.*, 1962, **260**, p 230-240
85. A. Bergstein and P. Kleinert, Partial Phase Diagram of the System $Mn_xFe_{3-x}O_y$, *Coll. Czech. Chem. Commun.*, 1964, **29**, p 2549-2551
86. D.G. Wickham, The Chemical Composition of Spinels in the System Fe_3O_4-Mn_3O_4, *J. Inorg. Nucl. Chem.*, 1969, **31**, p 313-320
87. Y.V. Golikov, S.A. Petrova, R.G. Zakharov, V.K. Antonov, and V.F. Balakirev, Equilibrium and Unstable States of the Fe-Mn-O System in Air, *Russ. J. Inorg. Chem.*, 1996, **41**, p 1510-1513
88. S.A. Petrova, Y.V. Golikov, R.G. Zakharov, and V.F. Balakirev, Heterogeneous Equilibria in the Fe-Mn-O System in Air, *Russ. J. Phys. Chem.*, 1997, **71**, p 184-186
89. B. Mason, Mineralogical Aspects of the System FeO-Fe_2O_3-MnO-Mn_2O_3, *Geol. Fören. Stockholm Förh.*, 1943, **65**, p 97-180
90. V.A.M. Brabers, Cation Migration, Cation Valencies and the Cubic-Tetragonal Transition in $Mn_xFe_{3-x}O_4$, *J. Phys. Chem. Solids*, 1971, **32**, p 2181-2191
91. P. Holba, M.A. Khilla, and S. Krupicka, On the Miscibility Gap of Spinels $Mn_xFe_{3-x}O_{4+\gamma}$, *J. Phys. Chem. Solids*, 1973, **34**, p 387-395
92. H.F. McMurdie, B.M. Sullivan, and F.A. Mauer, High Temperature X-Ray Study of the System Fe_3O_4-Mn_3O_4, *J. Res. Nat. Bur. Stand.*, 1950, **45**, p 35-41
93. J.M. Hastings and L.M. Corliss, Neutron Diffraction Study of Manganese Ferrite, *Phys. Rev.*, 1956, **104**, p 328-331
94. S. Krupicka and K. Zaveta, The Distribution of Ions and their Valencies in Manganese Ferrites I. $MnFe_2O_{4+\gamma}$ Ferrites, *Czech. J. Phys.*, 1959, **9**, p 324-331
95. G.A. Sawatzky, F. Van Der Woude, and A.H. Morrish, Note on Cation Distribution of $MnFe_2O_4$, *Phys. Lett.*, 1967, **25A**, p 147-148
96. T. Yamanaka and M. Nakahira, Dependence of the Cation Distribution in Manganese Ferrite on Temperature and Oxidation, *Mineral. J.*, 1973, **7**, p 202-220
97. Z. Jirák and S. Vratislav, Temperature Dependence of Distribution of Cations in $MnFe_2O_4$, *Czech. J. Phys.*, 1974, **24**, p 642-647
98. M. Rotter, B. Sedlák, Z. Simsa, and V.A.M. Brabers, NMR Study of Valency States in $MnFe_2O_4$, *Phys. Stat. Sol.*, 1977, **40**, p K169-K171
99. B. Gillot, M. Laarj, S. Kacim, T. Battault, R. Legros, and A. Rousset, Cationic Distribution and Oxidation Kinetics of Divalent Manganese Ions in Iron Manganite Spinels $Mn_{3-x}Fe_xO_4$ ($0 < x < 1.50$), *Solid State Ionics*, 1996, **83**, p 215-223
100. K. Terayama, M. Ikeda, and M. Taniguchi, Phase Equilibria in the Mn-Fe-O System in CO_2-H_2 Mixtures, *Trans. Jpn. Inst. Met.*, 1983, **24**, p 514-517
101. L.A. Reznitskii, Heat Capacity, Enthalpy and Entropy of Manganese Ferrite ($MnFe_2O_4$) in the 298-1000 K Range, *Izv. Akad. Nauk SSSR Neorg. Mater.*, 1974, **10**, p 477-480
102. K. Naito, H. Inaba, and H. Yagi, Heat Capacity Measurements of $Mn_xFe_{3-x}O_4$, *Solid State Chem.*, 1981, **36**, p 28-35

103. S.E. Harrison, C.J. Kriessman, and S.R. Pollack, Magnetic Spectra of Manganese Ferrites, *Phys. Rev.*, 1958, **110**, p 844-849
104. V.L. Moruzzi, Triangular Moment Arrangements in Manganese-Iron Spinels, *J. Appl. Phys. Sci.*, 1961, **32**, p 59-61
105. R. Gerber, Z. Simsa, and M. Vichr, Some Physical Properties of Single Crystal Manganese Ferrites, *Czech. J. Phys. Ser. B*, 1966, **16**, p 913-918
106. R. Buhl, Manganites spinelles purs d'elements de transition preparations et structures cristallographiques, *J. Phys. Chem. Solids*, 1969, **30**, p 805-812
107. U. Nölle, "Gleichgewichtsuntersuchungen im System Eisen-Mangan-Sauerstoff," Doctoral Thesis, Technische Universität Berlin, 1974
108. D. Janke and W.A. Fischer, Gleichgewichte von Chrom und Mangan mit Sauerstoff in Eisenschmelzen bei 1600°C, *Arch. Eisenhuttenw.*, 1976, **47**, p 147-151
109. D.C. Hilty and W. Crafts, Solubility of Oxygen in Liquid Iron Containing Silicon and Manganese, *Trans. Met. Soc. AIME*, 1959, **188**, p 425-436
110. S.M. Averbukh and L.A. Smirnov, Equilibrium Between Manganese and Oxygen in Molten Iron, *Steel in the USSR*, 1981, **13**, p 123-126
111. V.P.M. Mathew, M.L. Kapoor, and M.G. Frohberg, Untersuchungen zum Mangan-Sauerstoff-Gleichgewicht im flüssigen Eisen bei 1600°C, *Arch. Eisenhuttenw.*, 1972, **43**, p 865-872
112. V.E. Shevtsov, E.E. Merker, and V.P. Luzgin, Oxygen Solubility in High Manganese Iron Melts, *Steel in the USSR*, 1987, **17**, p 393-394
113. P. Oberhoffer and H. Schenck, Theoretische und Experimentelle Untersuchungen über die Desoxydation der Eisen mit Mangan, *Stahl u. Eisen*, 1927, **47**, p 1526-1530
114. W. Oelsen and G. Heynert, Die Reaktionen zwischen Eisen-Mangan-Schmelzen und den Schmelzen ihrer Aluminate, *Arch. Eisenhuttenw.*, 1955, **26**, p 567-575
115. J.-O. Andersson, T. Helander, L. Höglund, P. Shi, and B. Sundman, Thermo-Calc & DICTRA, Computational Tools for Materials Science, *CALPHAD*, 2002, **26**, p 273-312
116. A. Dinsdale, SGTE Data for Pure Elements, *CALPHAD*, 1991, **15**, p 317-425
117. R.J. Hill, J.R. Craig, and G.V. Gibbs, Systematics of the Spinel Structure Type, *Phys. Chem. Miner.*, 1979, **4**, p 317-339
118. G.D. Rieck and F.C.M. Driessens, The Structure of Manganese-Iron-Oxygen Spinels, *Acta Cryst.*, 1966, **20**, p 521-525
119. G.D. Murthy, L.M. Rao, R.J. Begum, M.G. Natera, and S.I. Youssef, Neutron Scattering Studies of Some Spinels, *J. de Phys.*, 1971, **32**(Suppl C1), p 318-319
120. J. Faller and C.E. Birchenall, The Temperature Dependence of Ordering in Magnesium Ferrite, *J. Appl. Cryst.*, 1970, **3**, p 496-503
121. J.D. Tretjakov, Y.G. Saksonov, and I.V. Gordeev, Phase Diagram of the System Fe_3O_4-Mn_3O_4-MnO-FeO at 1000°C and Thermodynamic Properties of the Coexisting Phases, *Inorg. Mater.*, 1965, **1**, p 382-386
122. H. Mao, M. Hillert, M. Selleby, and B. Sundman, Thermodynamic Assessment of the CaO-Al_2O_3-SiO_2 System, *J. Am. Ceram. Soc.*, 2006, **89**, p 298-308
123. H. Mao, O. Fabrichnaya, M. Selleby, and B. Sundman, Thermodynamic Assessment of the MgO-Al_2O_3-SiO_2 System, *J. Mater. Res.*, 2005, **20**, p 975-986